U.S. DEPARTMENT OF COMMERCE
National Technical Information Service

PB-260 136

MASS TRANSPORT MECHANISMS IN OPEN-CHANNEL FLOW

VANDERBILT UNIVERSITY, NASHVILLE, TENNESSEE

1966

C01715 253167 PB 260 136

MASS TRANSPORT MECHANISMS IN OPEN-CHANNEL FLOW

JAMES R. HAYS
PETER A. KRENKEL
KARL B. SCHNELLE, JR.

TECHNICAL REPORT NUMBER 8

Sanitary and Water Resources Engineering
Department of Civil Engineering
Vanderbilt University
Nashville, Tennessee

1966

REPRODUCED BY
NATIONAL TECHNICAL
INFORMATION SERVICE
U. S. DEPARTMENT OF COMMERCE
SPRINGFIELD, VA. 22161

BIBLIOGRAPHIC DATA SHEET	1. Report No.	2.	3. Recipient's Accession No. PB-260 136
4. Title and Subtitle Mass Transport Mechanisms in Open-Channel Flow.			5. Report Date 1966 6.
7. Author(s) James R. Hays, Peter A. Krenkel, and Karl B. Schnelle, Jr.			8. Performing Organization Rept. No. TR-8
9. Performing Organization Name and Address Vanderbilt Univ., Nashville, Tenn. Dept of Sanitary and Water Resources Engineering.*			10. Project/Task/Work Unit No. 11. Contract/Grant No. PHS-WP-ØØ328
12. Sponsoring Organization Name and Address *Public Health Service, Washington, D. C.			13. Type of Report & Period Covered Technical rept. 14.

15. Supplementary Notes

16. Abstracts

This investigation develops a description of mass transport in streams and rivers that is readily soluble and yet retains the basic mass transport mechanisms. The resulting model--the dead zone model--is developed from a logical simplification of the basic mass transport equation, is superior to the dispersed flow model, and does not suffer from the shortcomings of the complete descriptions. The superiority of the dead zone model over the dispersed flow model is demonstrated by comparing the ability of the models to predict the spread of inert tracer in channels and rivers, and applications are discussed.

17. Key Words and Document Analysis. 17a. Descriptors

17b. Identifiers/Open-Ended Terms

*Water flow
Hydrology
*Mathematical models
Water pollution
Rivers
Streams

17c. COSATI Field/Group 13B

18. Availability Statement	19. Security Class (This Report) UNCLASSIFIED	21. No. of Pages 147
	20. Security Class (This Page UNCLASSIFIED	22. Price

FORM NTIS-35 (REV. 10-73) ENDORSED BY ANSI AND UNESCO. THIS FORM MAY BE REPRODUCED USCOMM-DC 8265-P74

MASS TRANSPORT MECHANISMS IN OPEN-CHANNEL FLOW

JAMES R. HAYS
PETER A. KRENKEL
KARL B. SCHNELLE, JR.

TECHNICAL REPORT NUMBER 8

Sanitary and Water Resources Engineering
Department of Civil Engineering
Vanderbilt University
Nashville, Tennessee
1966

ACKNOWLEDGMENTS

Sincerest appreciation is expressed to Dr. K. B. Schnelle, Jr., and Dr. P. A. Krenkel for their guidance and advice during the course of this work.

This investigation was partially supported by the United States Public Health Service through Research Grant Number WP-00328 and by the National Aeronautics and Space Administration in the form of a Scholarship Grant.

Personal thanks are expressed to Mrs. Virginia Lester, Dr. Bill Clements, and Dr. Ed Thackston.

TABLE OF CONTENTS

		Page
ACKNOWLEDGMENTS	. . . . .	ii
LIST OF FIGURES	. . . . .	v
LIST OF TABLES	. . . . .	vi
Chapter		
I	INTRODUCTION	1
II	TURBULENT MASS TRANSFER	5
III	ONE DIMENSIONAL APPROXIMATIONS	10
	The Dispersed Flow Model	10
IV	THE DEAD ZONE MODEL	14
	Dispersed Flow Model Deficiencies	14
	The Dead Zone Concept	16
	Development of the Dead Zone Model Equations	18
	Perfectly Mixed Dead Zone	20
	Lateral Diffusion Dead Zone	22
V	SOLUTION OF THE DEAD ZONE EQUATIONS	35
	Measured Input, Perfectly Mixed Dead Zone	35
	Dimensionless Groups	37
	Distributed Concentration Measurements	44
	Rapid Injection, Perfectly Mixed Dead Zone	45
	Inversion	48
	Solutions for Diffusive Dead Zone Models	50
	Dead Zone Solution Characteristics	54

Page

Chapter

V (Continued)

Reduction to the Dispersed Flow Model 55
Interpretation of the Dead Zone Concentration-time Curves 57
Moments 60

VI CHANNEL EXPERIMENTS 63

VII RIVER EXPERIMENTS 79

VIII CONCLUSIONS 85

APPENDICES 91

A FREQUENCY DOMAIN MODEL EVALUATION 92

The Least Squares Criterion 92
Fourier Transforms for Real Functions 93
Transformation of the Least Squares Criterion to the Frequency Domain 94
Numerical Fourier Transformation 95
Numerical Fourier Inversion 98
Example of Frequency Domain Model Evaluation 100
Advantages of Frequency Domain Modeling 105
Conclusions 108
Nomenclature for Appendix A 108

B MODEL-PROTOTYPE SCALE RELATIONS 110

Nomenclature for Appendix B 114

C DISPERSED FLOW AND DEAD ZONE MODEL PARAMETERS: CHANNEL EXPERIMENTS 115

D DISPERSED FLOW AND DEAD ZONE MODEL PARAMETERS: RIVER EXPERIMENTS 128

E NOMENCLATURE 132

LIST OF REFERENCES 136

LIST OF FIGURES

Figure		Page
1	TYPICAL DISPERSED FLOW PREDICTIONS	15
2	DEAD ZONE SCHEMATIC	17
3	DEAD ZONE CROSS SECTIONS	25
4	RAPID INJECTION SOLUTION OF PERFECTLY MIXED DEAD ZONE MODEL	58
5	INJECTION APPARATUS	64
6	CONDUCTIVITY PROBES	66
7	STANDARD BRICK ARRANGEMENTS	69
8	SPECIAL BRICK ARRANGEMENTS	70
9	F STATISTIC FOR CHANNEL TESTS	74
10	F STATISTIC FOR CHANNEL TESTS	75
11	F STATISTIC FOR CHANNEL TESTS	76
12	DISPERSED FLOW AND DEAD ZONE MODEL FITS . .	77
13	F STATISTIC FOR RIVER TESTS	84
14	PREDICTION OF THE DISPERSION COEFFICIENT . .	89
15	RESPONSE OF 1/(Ts + 1) TO A TRIANGULAR PULSE	102

LIST OF TABLES

Table		Page
1	DIFFERENTIAL EQUATIONS OF DEAD ZONE MODELS .	26
2	TRANSFORMED EQUATIONS	27
3	DEAD ZONE TRANSFORMED SOLUTIONS	28
4	ALTERNATE FORM OF TRANSFORMED EQUATIONS . . .	29
5	SERIES EXPANSIONS OF TRANSFER FUNCTIONS . . .	30
6	TRANSFER FUNCTIONS REFORMED	31
7	TRANSFORMED SOLUTIONS	32
8	DEAD ZONE MODEL PARAMETERS	33
9	DISTRIBUTION DEFINITIONS	34
10	TYPICAL COMPARISONS OF MODEL PARAMETERS: CHANNEL EXPERIMENTS	72
11	CALCULATIONS OF RESPONSE DISCONTINUITIES . .	103

CHAPTER I

INTRODUCTION

The recognition of clean water as one of mankind's important natural resources has been long delayed due simply to its abundance. The value of this resource and its rapidly decreasing supply appear to have been simultaneously discovered. In this country, the suddenness of this discovery has hidden the fact that it is not water that is in short supply, but clean water. Extensive publicity has been given to schemes to produce fresh water from sea water. However, such schemes are not economically competitive with the more basic solution to the problem; i.e., the prevention of pollution and the cleaning of polluted water (19). Even the prospect of inexpensive nuclear power does not swing the balance, and conservation of fresh water is man's best source of fresh water (19).

In order to explain the interaction of pollutants and the fresh water environment, it is necessary for the engineer to draw information from such diverse fields as Biology, Mathematics, Chemistry, etc. However, basic to

any such explanation is an adequate description of the mass transport of inert pollutants by rivers and streams. Due to the pressing need for a stopgap characterization of the complete problem, some investigators have been forced to accept deficient or erroneous descriptions of the mass transport problem. This investigation will be concerned with the suitability of the mass transport descriptions now in use and the development of more adequate descriptions.

Modern investigators approach the subject of turbulent mass transfer with some reservation. Bird (3), at the beginning of his chapter on concentration distributions in turbulent flow, says, "Here we turn our attention to turbulent mass transport, a subject about which not a great deal can be said at the present time." However, concerning the application of turbulent mass transport theory to rivers and streams one thing can be said. The complexity and variety of the geometry and hydrodynamics of rivers indicates that some rigor will have to be sacrificed to obtain a soluble description. "Quite often, a simpler mathematical model based upon sounder premises will yield far more than a quite sophisticated mathematical model based upon a less firm foundation. Approximation, after all, may be made in

two places - in the construction of the model and in the solution of the associated equations. It is not at all clear which yields a more judicious approximation" (2).

It does seem clear that neither of the two common approaches to mass transfer in streams and rivers is a suitable compromise between simplicity and sophistication. The one dimensional dispersed flow model is far too simple an approach. Abundant evidence exists of its deficiencies (10, 15). The attempts to solve the complete three dimensional description by Monte Carlo or finite difference techniques are too sophisticated (4, 28). They suffer not only from lengthy calculational procedures, but also require detailed velocity and turbulent diffusivity profiles.

In this investigation, a description of mass transport in streams and rivers that is readily soluble and yet retains the basic mass transport mechanisms is developed. This model is superior to the dispersed flow model in its characterization of mass transport, and it does not suffer from the shortcomings of the complete descriptions. It is referred to as the dead zone model.

The dead zone model is developed from a logical

simplification of the basic mass transport equation presented in Chapter I. The superiority of the dead zone model over the dispersed flow model is demonstrated by comparing the ability of the models to predict the spread of inert tracer in channels and rivers. Applications of the dead zone model are discussed in the final chapter.

CHAPTER II

TURBULENT MASS TRANSFER

The Eulerian form of the equation of continuity for dilute liquid solutions of constant density and diffusivity is

$$\frac{\partial c}{\partial t} = D^m\left(\frac{\partial^2 c}{\partial x^2} + \frac{\partial^2 c}{\partial y^2} + \frac{\partial^2 c}{\partial z^2}\right) - \left(\frac{\partial v_x c}{\partial x} + \frac{\partial v_y c}{\partial y} + \frac{\partial v_z c}{\partial z}\right) \qquad (2\text{-}1)$$

Only two transport mechanisms are involved here; the velocity transport and molecular diffusion according to Fick's law. In the above form, this equation is not suitable for the analysis of mass transport in turbulent flow. Knowledge of the time and space varying velocity vector is not available. Furthermore, there is evidence that this rapidly oscillating vector is best described as a statistical quantity (3). The same reasoning can be applied to concentration fluctuations. These considerations suggest that the concentration and the velocity vector be replaced by a time-smoothed value plus a term to describe the fluctuations.

Thus,

$$c = \bar{c} + c' \tag{2-2}$$

$$v_x = \bar{v}_x + v'_x \tag{2-3}$$

Substitution of these relations in the equation of continuity and time averaging gives

$$\frac{\partial \bar{c}}{\partial t} = D^m \left(\frac{\partial^2 \bar{c}}{\partial x^2} + \frac{\partial^2 \bar{c}}{\partial y^2} + \frac{\partial^2 \bar{c}}{\partial z^2} \right)$$

$$- \left(\frac{\partial \bar{v}_x \bar{c}}{\partial x} + \frac{\partial \bar{v}_y \bar{c}}{\partial y} + \frac{\partial \bar{v}_z \bar{c}}{\partial z} \right)$$

$$- \left(\frac{\partial \overline{v'_x c'}}{\partial x} + \frac{\partial \overline{v'_y c'}}{\partial y} + \frac{\partial \overline{v'_z c'}}{\partial z} \right) \tag{2-4}$$

The time averaged concentrations and velocities have replaced the concentrations and velocities in Equation 2-1, but new terms, analogous to Reynolds stresses in momentum transport, have arisen. These terms may be referred to as turbulent mass fluxes. The analogy is not perfect, however, since Reynolds stresses involve a product of two vectors, whereas these terms involve a vector-scalar product.

In order to solve Equation 2-4 it is necessary to formulate a relationship between the turbulent mass flux and the time-smoothed concentration. Theoretical considerations produce no unique answer and a number of semiempirical expressions are available (3). Each expression produces certain difficulties in application. The formulation of von Karman is awkward and difficult to solve, Prandtl's mixing length varies with position and also presents integration problems, and the eddy diffusivity is a function of position. However, there are certain advantages in using the turbulent or eddy diffusivity analogy to Fick's molecular diffusion. If the following expressions for eddy diffusivity

$$\overline{v'_x c'} = D^t \frac{\partial \bar{c}}{\partial x}$$

$$\overline{v'_y c'} = D^t \frac{\partial \bar{c}}{\partial y}$$

$$\overline{v'_z c'} = D^t \frac{\partial \bar{c}}{\partial z} \qquad (2\text{-}5)$$

are substituted into Equation 2-4, there results

$$\frac{\partial c}{\partial t} = D^m \left(\frac{\partial^2 c}{\partial x^2} + \frac{\partial^2 c}{\partial y^2} + \frac{\partial^2 c}{\partial z^2} \right)$$

$$+ \frac{\partial}{\partial x} D^t \frac{\partial c}{\partial x} + \frac{\partial}{\partial y} D^t \frac{\partial c}{\partial y} + \frac{\partial}{\partial z} D^t \frac{\partial c}{\partial z}$$

$$- \left(\frac{\partial v_x c}{\partial x} + \frac{\partial v_y c}{\partial y} + \frac{\partial v_z c}{\partial z} \right) \qquad (2\text{-}6)$$

Note that the bars above c and v have been dropped for convenience. One of the advantages of using an eddy diffusivity expression for the turbulent mass flux is now apparent, since the molecular and turbulent diffusivities are additive as shown by the equation

$$\frac{\partial}{\partial x} (D^m + D^t) \frac{\partial c}{\partial x} = D^m \frac{\partial^2 c}{\partial x^2} + \frac{\partial}{\partial x} D^t \frac{\partial c}{\partial x} \qquad (2\text{-}7)$$

Thus, Equation 1-6 becomes

$$\frac{\partial c}{\partial t} = \frac{\partial}{\partial x} D^{mt} \frac{\partial c}{\partial x} + \frac{\partial}{\partial y} D^{mt} \frac{\partial c}{\partial y} + \frac{\partial}{\partial z} D^{mt} \frac{\partial c}{\partial z}$$

$$- \left(\frac{\partial v_x c}{\partial x} + \frac{\partial v_y c}{\partial y} + \frac{\partial v_z c}{\partial z} \right) \qquad (2\text{-}8)$$

where $D^{mt} = D^m + D^t$

Equation 2-8 should be considered to be the point of departure for simplifications of turbulent mass transport

problems. For many applications $v_y = v_z = 0$ and v_x is not a function of x. Thus, Equation 1-8 becomes

$$\frac{\partial c}{\partial t} = \frac{\partial}{\partial x} D^{mt} \frac{\partial c}{\partial x} + \frac{\partial}{\partial y} D^{mt} \frac{\partial c}{\partial y} + \frac{\partial}{\partial z} D^{mt} \frac{\partial c}{\partial z} - v_x \frac{\partial c}{\partial x} \qquad (2\text{-}9)$$

CHAPTER III

ONE DIMENSIONAL APPROXIMATIONS

The turbulent transport Equation 2-9 is formidable in application, and it is only natural that earlier investigators would select the simple geometry of the pipe on which to focus their efforts. For pipe flow, the transport equation can be written in cylindrical coordinates as

$$\frac{\partial c}{\partial t} = \frac{1}{r} \frac{\partial}{\partial r} \left(r D^{mt} \frac{\partial c}{\partial r} \right) + D^{mt} \frac{\partial^2 c}{\partial x^2} - v_x \frac{\partial c}{\partial x} \qquad (3\text{-}1)$$

where r is the radial coordinate. This equation is restricted to zero velocity components in the radial and angular directions and no concentration gradients in the angular direction. The velocity, v_x, and the diffusivity, D^{mt}, are a function of r only.

The Dispersed Flow Model

G. I. Taylor (24, 25), in 1954, sought to circumvent the difficulties of solving Equation 3-1 by considering only the cross-sectional average concentration. He used empirical expressions for velocity and the Reynolds analogy to define

the variation of v_x and D^t with r through heuristic arguments he concluded that the transport mechanisms described by Equation 3-1 could be represented by the one dimensional form,

$$\frac{\partial c}{\partial t} = D \frac{\partial^2 c}{\partial x^2} - U \frac{\partial c}{\partial x} \qquad (3\text{-}2)$$

where c represents the cross-sectional average concentration, U is the average longitudinal velocity, and D is a virtual coefficient of diffusion, more commonly called the longitudinal mixing coefficient or dispersion coefficient. Equation 3-2 is referred to as the dispersed flow model. A relation between D and the stress at the wall, τ_o, was given by Taylor as

$$D = 10.06\, R(\tau_o/\rho)^{\frac{1}{2}} \qquad (3\text{-}3)$$

where R is the radius and ρ is the fluid density.

In 1956, Aris (1) rigorously developed the relationship between Equation 3-1 and the dispersed flow model. He showed that Equation 3-3 is actually the result of equating the rate of change of the second moments of the distributions described by Equations 3-1 and 3-2. In addition, he derived a general method to obtain the second moment of Equation 2-9 for an arbitrary cross-sectional geometry.

A number of attempts have been made to apply the methods of Taylor and Aris to stream flow. Some investigators (21, 22) attempted to use Taylor's expression for D directly, calculating τ_o from the rate of energy expenditure and using a hydraulic radius for R. Such applications are incorrect since there is no relation between the geometry or velocity distributions in stream flow and those occurring in a pipe. Elder (10) assumed that only the vertical velocity gradient is important in stream flow and developed an expression analogous to Taylor's (Equation 3-3) but with the coefficient equal to 5.93. Other investigators (27, 28) have derived similar expressions for D based upon various assumptions.

Fischer (11) compared the predictions of some of the above expressions with the results of experimental laboratory and stream data. He found a large range in the values of the dispersion coefficient, and in general the value was many times greater than predicted. A number of possible explanations were considered and he concluded that lateral non-uniformity was the most important. The application of Aris' method to assumed lateral velocity profiles showed that

lateral velocity gradients . . . can easily overwhelm all other effects in causing longitudinal dispersion" (11). Fischer further showed that the dispersion coefficient is extremely sensitive to the form of the velocity profile and suggested that successful predictions of D may have to be based upon detailed experimental knowledge of the velocity profiles.

CHAPTER IV

THE DEAD ZONE MODEL

Dispersed Flow Model Deficiencies

The shortcomings of a one dimensional representation of the mixing phenomena are not limited to an inability to predict D. Many investigators have noted that the dispersion model does not adequately explain experimental results. The deviations are always of the same form. The predicted distribution is normal with respect to distance while observed results are skewed, having long tails on the trailing portions and truncated leading edges. The effect of this deviation on a typical time-concentration record is shown in Figure 1.

Taylor (25) observed this phenomenon at low Reynolds numbers in pipes, and attributed it to a significant laminar layer which was not considered in his theory. Elder (10) observed the same thing in experiments in laboratory models of stream flow. He also postulated a laminar sublayer and made a quantitative attempt to describe this effect. Krenkel (15) commented on long tails in general and suggested

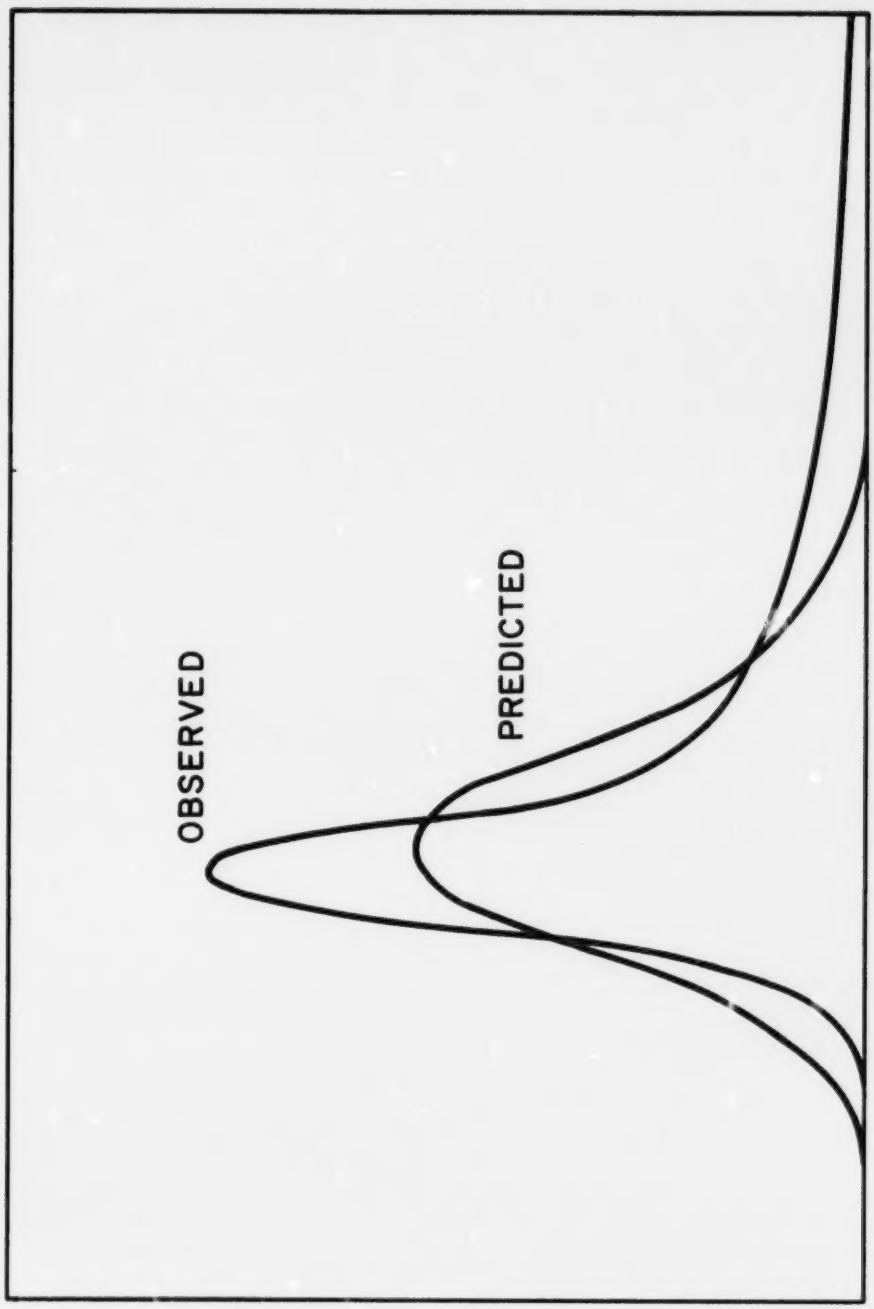

FIGURE 1 TYPICAL DISPERSED FLOW PREDICTIONS

that relatively stagnant regions contribute to the effect. Fisher (11) points out that "Stagnant areas along the banks, caused by debris, unevenness of the banks, etc., are also common . . . "

The Dead Zone Concept

All these comments imply that a better description of the spread of material in streams and rivers could be formulated if a typical cross section was considered to consist of two distinct zones: a main stream and a stagnant or dead zone. Figure 2 depicts this concept. In the main stream the dominant mass transport mechanisms are longitudinal and lateral turbulent diffusion impressed upon a velocity profile with relatively weak gradients. Thus, many of the effects that cause deviation from the one dimensional dispersed flow model have been isolated from this zone and it should be adequately described by such a model. In the dead zone, longitudinal velocity is essentially zero, and lateral mass transport is the only important mechanism. While some longitudinal transport may be present in the dead zone, it is negligible compared to such transport in the main stream. Also, note that the interface between the main stream and dead zone simulates the sharp

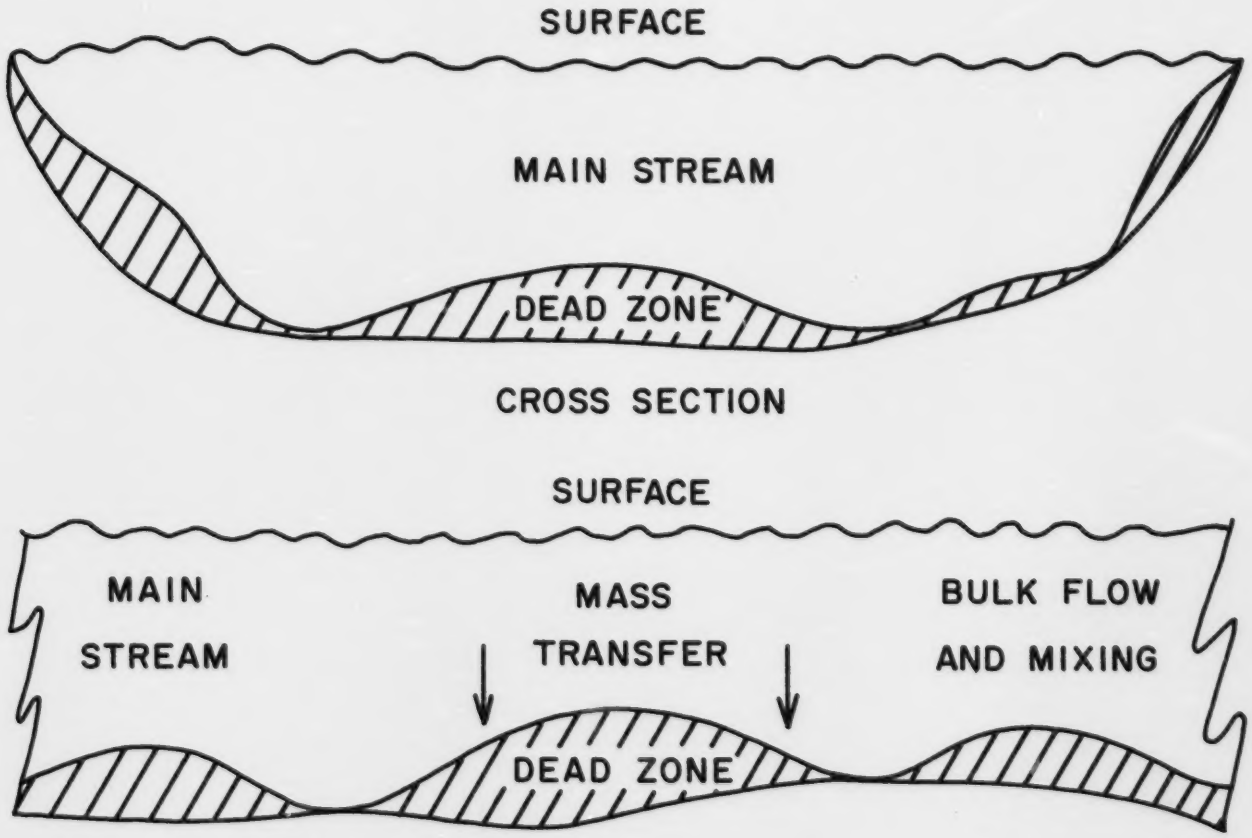

FIGURE 2 DEAD ZONE SCHEMATIC

velocity gradients characteristic of turbulent velocity profiles near the banks of streams and rivers.

It is not clear, at this point, what form the lateral mass transfer mechanism within the dead zone should take. It may be satisfactory to assume uniform concentration within a given dead zone cross section. This is tantamount to saying that any dead zone cross section is perfectly mixed. For this description it is appropriate to assume that mass transfer is proportional to the difference in the average concentration in the main stream and the concentration in the dead zone.

However, the perfectly mixed dead zone cross section may be too crude a description. A more sophisticated approach would be to consider that material must diffuse laterally in and out of the dead zone according to the time-varying concentration at the interface. In this case, the geometry of the dead zone must be specified in order to establish the rate at which material is exchanged between the main stream and the dead zone.

Development of the Dead Zone Model Equations

The differential equations describing the dead zone model are obtained by incorporating the physical description

of the previous section into a mass balance.

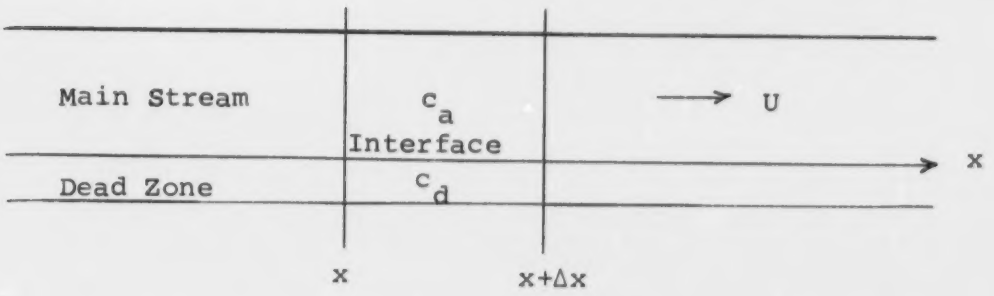

Referring to the above diagram the following mass balance can be made across the section x to x + Δx:

$$\frac{d(c_a A_a \Delta x)}{dt} = A_a N_a\Big|_x - A_a N_a\Big|_{x+\Delta x} + A_a UC_a\Big|_x - A_a UC_a\Big|_{x+\Delta x} + \Delta x\, P\, N_d \qquad (4\text{-}1)$$

where x is longitudinal distance, A_a is the cross-sectional area of the main stream, P is the wetted contact length between the two zones, $P\Delta x$ is the contact area between the main stream and the dead zone, N_d is the rate of addition of mass to the main stream by the dead zone, and N_a is the rate of addition of mass by longitudinal dispersion. The term N_a can be written as

$$N_a = -D_a \frac{\partial c_a}{\partial x} \qquad (4\text{-}2)$$

Passing to the limit and making the above substitution gives

$$\frac{\partial c_a}{\partial t} = D_a \frac{\partial^2 c_a}{\partial x^2} - U \frac{\partial c_a}{\partial x} + \frac{P}{A_a} N_d \qquad (4\text{-}3)$$

This equation is generally valid for any dead zone mechanism, where N_d will be defined by a particular mechanism.

Perfectly Mixed Dead Zone

If it is assumed that a dead zone cross section is perfectly mixed as shown in Figure 3a, and mass transfer is proportional to the difference between the main stream and dead zone concentrations, then

$$N_d = K (c_d - c_a) \qquad (4\text{-}4)$$

where c_d is the dead zone concentration and K is the mass transfer coefficient. The differential equation for the dead zone concentration is straightforward.

$$\frac{\partial (c_d A_d)}{\partial t} = - PN_d = - KP (c_d - c_a) \qquad (4\text{-}5)$$

Thus, the simultaneous partial differential equations describing concentrations in both the main stream and dead zone can be written

$$\frac{\partial c_a}{\partial t} = D_a \frac{\partial^2 c_a}{\partial x^2} - U \frac{\partial c_a}{\partial x} + \frac{KP}{A_a} (c_d - c_a) \qquad (4\text{-}6)$$

$$\frac{\partial c_d}{\partial t} = \frac{KP}{A_d} (c_a - c_d) \qquad (4\text{-}7)$$

The conventional mass transfer group is usually written as Ka where a is the ratio of contact or wetted area to the volume of the main stream. It can be seen that

$$a = \frac{PL}{A_a L} = \frac{P}{A_a} \qquad (4\text{-}8)$$

where L is the length of the section under consideration. Similarly

$$d = \frac{PL}{A_d L} = \frac{P}{A_d} \qquad (4\text{-}9)$$

where d is the ratio of the contact area to the volume of the dead zone. Thus, Ka is the conventional mass transfer group based upon the volume of the main stream, and Kd is the mass transfer group based upon the volume of the dead zone. Equations 4-6 and 4-7 may be written

$$\frac{\partial c_a}{\partial t} = D_a \frac{\partial^2 c_a}{\partial x^2} - U \frac{\partial c_a}{\partial x} + Ka(c_d - c_a) \qquad (4\text{-}10)$$

$$\frac{\partial c_d}{\partial t} = Kd\,(c_a - c_d) \qquad (4\text{-}11)$$

Lateral Diffusion Dead Zone

If the mass transfer mechanism within the dead zone is considered to be lateral diffusion, the describing differential equation depends upon the dead zone geometry. Figures 3b, c, and d are schematics of three geometries that readily yield to analytical treatment. In the first case, the dead zone has a rectangular geometry characterized by parallel lines of mass flow. If the distance into the dead zone at any cross section is measured by y, and D_d is the diffusivity, then the differential equation is

$$\frac{\partial c_d}{\partial t} = D_d \frac{\partial^2 c_d}{\partial y^2} \qquad (4\text{-}12)$$

The rate at which material enters the main stream is given by

$$N_d = -D_d \left.\frac{\partial c_d}{\partial y}\right|_{y = L_d} \qquad (4\text{-}13)$$

where L_d is the depth of the dead zone and $y = L_d$ at the interface. Thus, the simultaneous equations describing a dead zone model with rectangular geometry are

$$\frac{\partial c_a}{\partial t} = D_a \frac{\partial^2 c_a}{\partial x^2} - U \frac{\partial c_a}{\partial x} - a D_a \left.\frac{\partial c_d}{\partial y}\right|_{y = L_d} \tag{4-14}$$

$$\frac{\partial c_d}{\partial t} = D_d \frac{\partial^2 c_d}{\partial y^2} \tag{4-15}$$

In the second case the dead zone has a cylindrical geometry characterized by converging lines of mass flow. The development of the differential equations for this dead zone model is quite similar to the previous case, and the equations may be written

$$\frac{\partial c_a}{\partial t} = D_a \frac{\partial^2 c_a}{\partial x^2} - U \frac{\partial c_a}{\partial x} - a D_d \left.\frac{\partial c_d}{\partial r}\right|_{r=R} \tag{4-16}$$

$$\frac{\partial c_d}{\partial t} = D_d \frac{\partial^2 c_d}{\partial r^2} + \frac{D_d}{r} \frac{\partial c_d}{\partial r} \tag{4-17}$$

where r is radial distance and R is the radius of the dead zone.

The dead zone has a spherical geometry in the third case and is characterized by lines of mass flow converging in three dimensions. Such a situation could not strictly occur within any given cross section, but for a relatively small dead zone radius it is a satisfactory representation.

Again the equation development is similar to the previous cases, and there results

$$\frac{\partial c_a}{\partial t} = D_a \frac{\partial^2 c_a}{\partial x^2} - U \frac{\partial c_a}{\partial x} - a D_d \left.\frac{\partial c_d}{\partial r}\right|_{r=R} \qquad (4\text{-}18)$$

$$\frac{\partial c_d}{\partial t} = D_d \frac{\partial^2 c_d}{\partial x^2} + \frac{2 D_d}{r} \frac{\partial c_d}{\partial r} \qquad (4\text{-}19)$$

Table 1 summarizes the differential equations describing the various dead zone models. The similarity between models could be better demonstrated with a slight modification of form, but this is more easily accomplished upon the transformed equations, and will be shown later. In the next section basic solutions to all dead zone models will be developed.

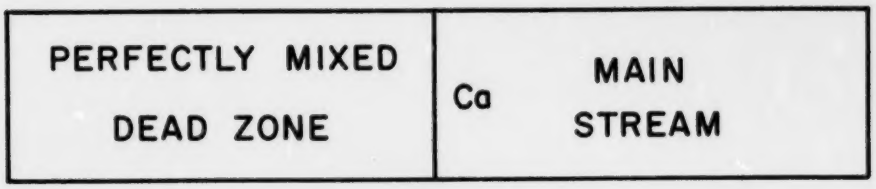

3a

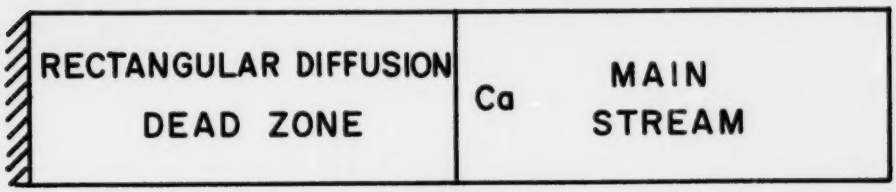

3b

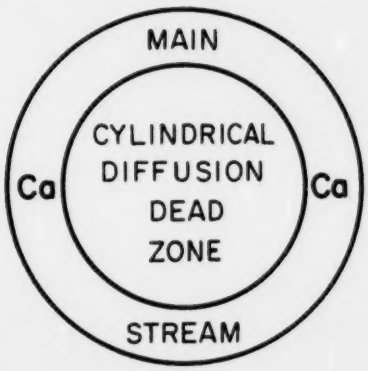

3c

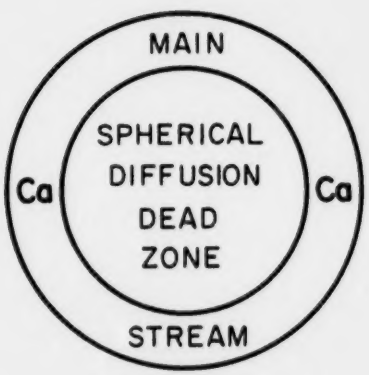

3d

FIGURE 3 DEAD ZONE CROSS SECTIONS

TABLE 1 DIFFERENTIAL EQUATIONS OF DEAD ZONE MODELS

PERFECTLY MIXED

$$\frac{\partial c_a}{\partial t} = D_a \frac{\partial^2 c_a}{\partial x^2} - U \frac{\partial c_a}{\partial x} + Ka\ (c_a - c_d)$$

$$\frac{\partial c_d}{\partial t} = Kd(c_a - c_d)$$

RECTANGULAR DIFFUSION

$$\frac{\partial c_a}{\partial t} = D_a \frac{\partial^2 c_a}{\partial x^2} - U \frac{\partial c_a}{\partial x} - a\ D_d \left.\frac{\partial c_d}{\partial y}\right|_{y=L_d}$$

$$\frac{\partial c_d}{\partial t} = D_d \frac{\partial^2 c}{\partial y^2}$$

CYLINDRICAL DIFFUSION

$$\frac{\partial c_a}{\partial t} = D_a \frac{\partial^2 c_a}{\partial x^2} - U \frac{\partial c_a}{\partial x} - a\ D_d \left.\frac{\partial c_d}{\partial r}\right|_{r=R}$$

$$\frac{\partial c_d}{\partial t} = D_d \frac{\partial^2 c_d}{\partial r^2} + \frac{D_d}{r} \frac{\partial c_d}{\partial r}$$

SPHERICAL DIFFUSION

$$\frac{\partial c_a}{\partial t} = D_a \frac{\partial^2 c_a}{\partial x^2} - U \frac{\partial c_a}{\partial x} - a\ D_d \left.\frac{\partial c_d}{\partial r}\right|_{r=R}$$

$$\frac{\partial c_d}{\partial t} = D_d \frac{\partial^2 c_d}{\partial r^2} + \frac{2D_d}{r} \frac{\partial c_d}{\partial r}$$

TABLE 2 TRANSFORMED EQUATIONS

PERFECTLY MIXED

$$D_a \frac{\partial^2 C_a}{\partial x^2} - U \frac{\partial C_a}{\partial x} - (Ka + s)\, C_a + Ka\, C_d = 0$$

$$(s + Kd)\, C_d = Kd\, C_a$$

RECTANGULAR DIFFUSION

$$D_a \frac{\partial^2 C_a}{\partial x^2} - U \frac{\partial C_a}{\partial x} - s\, C_a - a\, D_d \left.\frac{\partial C_d}{\partial y}\right|_{y=L_d} = 0$$

$$D_d \frac{\partial^2 C_d}{\partial y^2} - s\, C_d = 0$$

CYLINDRICAL DIFFUSION

$$D_a \frac{\partial^2 C_a}{\partial x^2} - U \frac{\partial C_a}{\partial x} - s\, C_a - a\, D_d \left.\frac{\partial C_d}{\partial r}\right|_{r=R} = 0$$

$$D_d \frac{\partial^2 C_d}{\partial r^2} + \frac{D_d}{r} \frac{\partial C_d}{\partial r} - s\, C_d = 0$$

SPHERICAL DIFFUSION

$$D_a \frac{\partial^2 C_a}{\partial x^2} - U \frac{\partial C_a}{\partial x} - s\, C_a - a\, D_d \left.\frac{\partial C_d}{\partial r}\right|_{r=R} = 0$$

$$D_d \frac{\partial^2 C_d}{\partial r^2} + \frac{2D_d}{r} \frac{\partial C_d}{\partial r} - s\, C_d = 0$$

TABLE 3 DEAD ZONE TRANSFORMED SOLUTIONS

PERFECTLY MIXED

$$C_d = \left(\frac{1}{s/Kd + 1}\right) C_a$$

RECTANGULAR DIFFUSION

$$C_d = \frac{\cosh(\sqrt{s/D_d}\, y)}{\cosh(\sqrt{s/D_d}\, L_d)} C_a$$

$$\left.\frac{\partial C_d}{\partial y}\right|_{y=L_d} = \sqrt{s/D_d}\, \tanh\sqrt{s/D_d}\, L_d)\; C_a$$

CYLINDRICAL DIFFUSION

$$C_d = \frac{I_o(\sqrt{s/D_d}\, r)}{I_o(\sqrt{s/D_d}\, R)} C_a$$

$$\left.\frac{\partial C_d}{\partial r}\right|_{r=R} = \sqrt{s/D_d}\quad \frac{I_1(\sqrt{s/D_d}\, R)}{I_o(\sqrt{s/D_d}\, R)}$$

SPHERICAL DIFFUSION

$$C_d = \frac{R}{r}\quad \frac{\sinh(\sqrt{s/D_d}\, r)}{\sinh(\sqrt{s/D_d}\, R)} C_a$$

$$\left.\frac{\partial C_d}{\partial r}\right|_{r=R} = (\sqrt{s/D_d}\, \coth(\sqrt{s/D_d}\, R) - 1/R)\; C_a$$

TABLE 4 ALTERNATE FORM OF TRANSFORMED EQUATIONS

ALL DEAD ZONE MODELS

$$\frac{\partial^2 C_a}{\partial x^2} - U \frac{\partial C_a}{\partial x} - \left[C_a + (A_d/A_a)\, C_{dav} \right] s = 0$$

$$C_{dav} = \Psi C_a$$

TABLE 5 SERIES EXPANSION OF TRANSFER FUNCTIONS

PERFECTLY MIXED

$$C_{dav} = \left(\frac{1}{s/Kd + 1}\right) C_a \qquad T_d = \frac{1/Kd}{T}$$

$$\psi = 1 - \frac{1}{Kd}\, s + \left(\frac{1}{Kd}\right)^2 s^2 - \ldots$$

RECTANGULAR DIFFUSION

$$C_{dav} = \frac{\tanh(\sqrt{s/D_d}\, L_d)}{\sqrt{s/D_d}\, L_d} C_a \qquad T_d = \frac{L_d^2/3D_d}{T}$$

$$\psi = 1 - \left(\frac{L_d^2}{3D_d}\right) s + \frac{6}{5}\left(\frac{L_d^2}{3D_d}\right) s^2 - \ldots$$

CYLINDRICAL DIFFUSION

$$C_{dav} = \frac{2\, I_1(\sqrt{s/D_d}\, R)}{\sqrt{s/D_d}\, R\, I_o(\sqrt{s/D_d}\, R)} C_a \qquad T_d = \frac{R^2/8D_d}{T}$$

$$\psi = 1 - \left(\frac{R^2}{8D_d}\right) s + \frac{4}{3}\left(\frac{R^2}{8D_d}\right)^2 s^2 - \ldots$$

SPHERICAL DIFFUSION

$$C_{dav} = 3\left(\frac{\coth(\sqrt{s/D_d}\, R)}{\sqrt{s/D_d}\, R} - \frac{1}{(s/D_d)\, R^2}\right) C_a \qquad T_d = \frac{R^2/15D_d}{T}$$

$$\psi = 1 - \left(\frac{R^2}{15D_d}\right) s + \frac{10}{7}\left(\frac{R^2}{15D_d}\right)^2 s^2 - \ldots$$

TABLE 6 TRANSFER FUNCTIONS REFORMED

PERFECTLY MIXED

$$\psi = 1 - T_d S + T_d^2 S^2 - \ldots$$

$$\psi = \frac{1}{T_d S + 1}$$

RECTANGULAR DIFFUSION

$$\psi = 1 - T_d S + \frac{6}{5} T_d^2 S^2 - \ldots$$

$$\psi = \frac{\tanh \sqrt{3T_d S}}{\sqrt{3T_d S}}$$

CYLINDRICAL DIFFUSION

$$\psi = 1 - T_d S + \frac{4}{3} T_d^2 S^2 - \ldots$$

$$\psi = \frac{2 I_1 \sqrt{8T_d S}}{\sqrt{8T_d S}\, I_o \sqrt{8T_d S}}$$

SPHERICAL DIFFUSION

$$\psi = 1 - T_d S + \frac{10}{7} T_d^2 S^2 - \ldots$$

$$\psi = 3 \left[\frac{\coth \sqrt{15T_d S}}{\sqrt{15\, T_d S}} - \frac{1}{15T_d S} \right]$$

TABLE 7 TRANSFORMED SOLUTIONS

MEASURED INPUT

$$\frac{C_{m1}}{C_{mo}} = \frac{\alpha_1 + \beta_1 \psi}{\alpha_o + \beta_o \psi} G$$

INJECTION INPUT

$$\frac{C_{m1}}{R_o/AU} = (\alpha_o + \beta_o \psi)(\alpha_1 + \beta_1 \psi) \frac{G}{\sqrt{1 + 2T(\alpha + \beta \psi)s}}$$

$$G = \exp\left[\left(1 - \sqrt{1 + 2T(\alpha + \beta\psi)s}\right)/T\right]$$

TABLE 8 DEAD ZONE MODEL PARAMETERS

$$T = \frac{\text{AVERAGE DISPERSION TRANSPORT RESIDENCE TIME IN MAIN STREAM}}{\text{AVERAGE VELOCITY TRANSPORT RESIDENCE TIME IN MAIN STREAM}}$$

$$T_d = \frac{\text{AVERAGE DEAD ZONE RESIDENCE TIME}}{\text{AVERAGE RESIDENCE TIME OF ENTIRE SECTION}}$$

α = MAIN STREAM FRACTION OF CROSS SECTION

β = DEAD ZONE FRACTION OF CROSS SECTION

$$\alpha + \beta = 1.0$$

T = AVERAGE RESIDENCE TIME OF ENTIRE SECTION

$$S = T_s$$

TABLE 9 DISTRIBUTION DEFINITIONS

α = MAIN STREAM FRACTION OF CROSS SECTION

β = DEAD ZONE FRACTION OF CROSS SECTION

$$\alpha + \beta = 1.0$$

α_o = FRACTION OF MEASUREMENT OR INJECTION MADE IN MAIN STREAM AT x = 0

β_o = FRACTION OF MEASUREMENT OR INJECTION MADE IN DEAD ZONE AT x = 0

$$\alpha_o + \beta_o = 1.0$$

α_1 = FRACTION OF MEASUREMENT MADE IN MAIN STREAM AT x = L

β_1 = FRACTION OF MEASUREMENT MADE IN DEAD ZONE AT x = L

$$\alpha_1 + \beta_1 = 1.0$$

CHAPTER V

SOLUTION OF THE DEAD ZONE EQUATIONS

Solutions for the perfectly mixed dead zone model will be considered initially and all the other cases will be treated simultaneously since they are quite similar. Tables 1 through 9 summarize the solutions and emphasize their similarity. It will be helpful in reading this chapter to refer to these tables often.

Measured Input, Perfectly Mixed Dead Zone

One important set of boundary conditions arises from an experiment in which a quantity of conservative tracer is introduced at some point along a stream, and the cross-sectional average concentration is measured in the main stream at two downstream points. The initial and boundary conditions for such an experiment can be written

I.C.	$t = 0$	$c_d(x,0) = 0$	
		$c_a(x,0) = 0$	(5-1)
B.C.	$x = 0$	$c_a(0,t) = c_{ao}(t)$	
	$x = \infty$	$c_a(x,t) = \text{Finite}$	(5-2)

Equations 4-10 and 4-11 are reproduced here.

$$\frac{\partial c_a}{\partial t} = D_a \frac{\partial^2 c_a}{\partial x^2} - U \frac{\partial c_a}{\partial x} + Ka\ (c_d - c_a) \qquad (4\text{-}10)$$

$$\frac{\partial c_d}{\partial t} = Kd\ (c_a - c_d) \qquad (4\text{-}11)$$

Laplace transformation gives

$$D_a \frac{\partial^2 C_a}{\partial x^2} - U \frac{\partial C_a}{\partial x} - (Ka + s)\ C_a + Ka\ C_d = 0 \qquad (5\text{-}3)$$

$$C_d = \frac{1}{s/Kd + 1} C_a \qquad (5\text{-}4)$$

Elimination of C_d yields

$$D_a \frac{\partial^2 C_a}{\partial x^2} - U \frac{\partial C_a}{\partial x} - \left(1 + \frac{A_d/A_a}{s/Kd + 1} \right) s\ C_a = 0 \qquad (5\text{-}5)$$

where the following relation was used.

$$\frac{Ka}{Kd} = \frac{a}{d} = \frac{P}{A_a} \frac{A_d}{P} = \frac{A_d}{A_a} \qquad (5\text{-}6)$$

The solution of Equation 5-5, after the application of the boundary conditions given by Equation 5-2, is

$$C_a = C_{ao} \exp\left[\left(U - \sqrt{U^2 + 4 D_a \left(1 + \frac{A_d/A_a}{s/Kd+1}\right) s} \right) \frac{x}{2 D_a} \right] \qquad (5\text{-}7)$$

Inversion of the above equation to give c_a will be postponed until a more general solution is found.

Dimensionless Groups

It is helpful to regroup the parameters into more basic combinations. One important parameter is the average residence time, T_d, of a particle entering the dead zone which can be found in this case from the impulse response by letting $C_a = 1.0$ in Equation 5-4. This represents a rapid introduction of material into the dead zone. The average residence time can be found from the first moment of the impulse response by evaluating $\left.\frac{dC_d}{ds}\right|_{s=0}$ and $C_d|_{s=0}$ as follows (16):

$$T_d = \frac{-\left.\frac{dC_d}{ds}\right|_{s=0}}{C_d|_{s=0}} = 1/Kd \qquad (5\text{-}8)$$

Two other parameters can be defined

$$\alpha = \frac{A_a}{A_a + A_d} \qquad \beta = \frac{A_d}{A_a + A_d} \tag{5-9}$$

where α represents the percent main stream volume, and β represents the percent dead zone volume. It is obvious that α plus β equals one.

Two parameters associated with the main stream can be defined. The first is the average residence time of a particle in the main stream in the absence of a dead zone and in the absence of longitudinal dispersion. In this case all particles have identical residence times. Thus,

$$T_v = L/U \tag{5-10}$$

where the subscript v refers to velocity transport. The second main stream parameter, T_{dp}, is a measure of the dispersive transport. It is defined as the average residence time of a particle in the main stream if it is transported by dispersion only. In order to find this time, it is necessary to impose the same restrictions that were automatically imposed in the definition of T_v, i.e., a particle is prevented from dispersing back "upstream"

after it has passed the planes x = 0 and x = L going "downstream." The differential equations and boundary conditions for this description are

$$\frac{\partial c}{\partial t} = D_a \frac{\partial^2 c}{\partial x^2} \tag{5-11}$$

$$\text{I.C.} \qquad t = 0 \qquad c(x,0) = (M/A_a)\,\delta(x) \tag{5-12}$$

$$\text{B.C.} \qquad x = 0 \qquad \frac{\partial c(0,t)}{\partial x} = 0$$

$$x = L \qquad c(L,t) = 0 \tag{5-13}$$

where M is the mass of material injected in the cross section A_a and $\delta(x)$ is the delta function. The initial condition given by Equation 5-12 represents a charge of tracer isolated in the plane x = 0 at time t = 0-. Laplace transformation of Equation 5-11 with respect to time gives

$$\frac{\partial^2 C}{\partial x^2} - (s/D_a)\,C = -(M/A_a D_a)\,\delta(x) \tag{5-14}$$

A second transformation with respect to distance gives

$$\bar{C} = \frac{-M/A_a D_a + B_p}{p^2 - s/D_a} \tag{5-15}$$

where p is the distance transform variable and B is an arbitrary constant. Inversion with respect to distance and application of boundary conditions yields

$$C = \frac{M/A_a D_a}{\sqrt{S/D_a}} \left[\tanh(\sqrt{s/D_a} L) \cosh \sqrt{s/D_a} x - \sinh(\sqrt{s/D_a} x) \right] \tag{5-16}$$

The average concentration in this section can be found by

$$C_{av} = (1/L) \int_o^L C \, dx \tag{5-17}$$

and the result is

$$C_{av} = \frac{M/A_a L}{s} \left(\frac{\cosh(\sqrt{s/D_a} L) - 1}{\cosh(\sqrt{s/D_a} L)} \right) \tag{5-18}$$

The first moment is more easily found if C_{av} is expanded in a series. The result is

$$T_{dp} = \frac{- \frac{dC_{av}}{ds} \Big|_{s=0}}{C_{av} \Big|_{s=0}} = \frac{5}{12} \frac{L^2}{D_a} \tag{5-19}$$

One final parameter is needed. It is the average residence time in the entire section, dead zone included, when all transport mechanisms are in effect. Spalding (23), in a general development, has shown this to be the ratio of the total volume to the flow rate. Thus,

$$T = \frac{L(A_a + A_d)}{UA_a} \tag{5-20}$$

Regrouping the parameters in Equation 5-7, at x = L C_a can be written

$$C_{a1} = C_{ao} \exp\left[\frac{L^2/2D_a}{L/U} \text{ times } \left(1 - \sqrt{1 + 2\left(\frac{L}{U}\frac{A_a + A_d}{A_a}\right)\left(\frac{A_a}{A_a+A_d} + \frac{A_d}{A_a+A_d} \frac{1}{s/Kd+1}\right)\left(\frac{L/U}{L^2/2\ D_a}\right)} \right)\right] \tag{5-21}$$

A dimensionless group can be replaced by the parameter, T, where

$$T = \frac{L/U}{L^2/2\,D_a} \tag{5-22}$$

The term $L^2/2D_a$ is almost equal to the average residence time, T_{dp}, defined by Equation 5-19. In view of the somewhat arbitrary manner in which the boundary conditions (Equations 5-12 and 5-13) were stipulated, it appears reasonable to neglect this slight difference and refer to T as the ratio of the average residence time by velocity transport alone to the average residence time by dispersion transport alone (in the main stream). In qualitative terms T is a measure of the relative importance of dispersive and velocity transport and can be called the relative dispersion coefficient. It is more common to replace the group in Equation 5-22 by 2/Pe where Pe is the Peclet number. However, the quantitative physical meaning associated with T is quite advantageous when dealing with numerical values. Another advantage is the straightforward dependence of the moments upon T (Equations 5-65, 5-66, and 5-67).

Using the definitions of T, T, α and β, which are summarized in Table 8, Equation 5-21 can be written

$$C_{a1} = C_{ao} \exp\left[\left(1 - \sqrt{1 + 2T(\alpha + \beta\psi)Ts}\right)/T\right] \qquad (5\text{-}23)$$

where ψ for the perfectly mixed dead zone is

$$\psi = \frac{1}{s/Kd + 1} \tag{5-24}$$

If the transform variable is redefined to include the average residence time of the entire system by writing $S = Ts$ then it is natural to define a term, T_d, as the ratio of the average residence time of the dead zone to the average residence time of the entire system.

$$T_d = T_d/T \tag{5-25}$$

Thus, at $x = L$, Equation 5-7 can be written

$$C_{al} = G\, C_{ao} \tag{5-26}$$

where

$$G = \exp\left[\left(1 - \sqrt{1 + 2T(\alpha + \beta\psi)S}\right)/T\right] \tag{5-27}$$

Table 8 summarizes the physical meaning of the dimensionless groups used in Equation 5-26 and 5-27. One final generalization needs to be made by writing Equation 5-4 as

$$C_d = \psi C_a \tag{5-28}$$

where

$$\psi = \frac{1}{T_d\, s+1} \tag{5-29}$$

Distributed Concentration Measurements

Equations 5-26 through 5-29 represent the main stream and dead zone transformed solutions when both measurements are made in the main stream. If measurements are made in both the main stream and the dead zone, the solution can be found in the following manner. At $x = 0$, let α_o represent the fraction of the measurement made in the main stream and let β_o represent the fraction of the measurement made in the dead zone. For example, if the measurement were made only in the main stream, $\alpha_o = 1$ and $\beta_o = 0$; if the measurement were made only in the dead zone, $\alpha_o = 0$ and $\beta_o = 1$; and if the measurement is made uniformly across the entire cross section, $\alpha_o = \alpha$ and $\beta_o = \beta$. At $x = L$, let the same respective quantities be called α_1 and β_1. Therefore, the measured concentration at $x = 0$ is

$$C_{mo} = \alpha_o\, C_{ao} + \beta_o\, C_{do} \tag{5-30}$$

which can be combined with Equation 5-28 to give

$$C_{mo} = (\alpha_o + \beta_o \psi)\ C_{ao} \tag{5-31}$$

In like manner the measured concentration at x = L can be written as

$$C_{m1} = (\alpha_1 + \beta_1 \psi)\ C_{a1} \tag{5-32}$$

Eliminating C_{ao} and C_{a1} from Equations 5-26, 5-31, and 5-32 gives

$$C_{m1} = \frac{\alpha_1 + \beta_1 \psi}{\alpha_o + \beta_o \psi}\ G\ C_{mo} \tag{5-33}$$

Equation 5-33 is the general transformed solution for concentration measurements made at x = 0 and x = L.

It is interesting to note that when both measurements are made only in the main stream, or only in the dead zone, or with the same distribution, Equation 5-33 becomes

$$C_{m1} = G\ C_{mo} \tag{5-34}$$

Rapid Injection, Perfectly Mixed Dead Zone

Another important set of boundary conditions is for the rapid injection of a quantity of tracer at x = 0 with the concentration measured at x = L. This is the most common

tracer testing technique for rivers and streams. The initial and boundary conditions can be written

$$\text{I.C.} \qquad t = 0 \qquad c_a(x,0) = \alpha_o (M/A_a)\ \delta(x)$$

$$c_d(x,0) = \beta_o (M/A_d)\ \delta(x) \qquad (5\text{-}35)$$

$$\text{B.C.} \qquad x = \infty \qquad c_a(x,0) = \text{Finite} \qquad (5\text{-}36)$$

where M is the total quantity of material injected and α_o and β_o now represent the fraction of M injected in the main stream and dead zone, respectively. Equations 4-10 and 4-11 are reproduced again for clarity.

$$\frac{\partial c_a}{\partial t} = D_a \frac{\partial^2 c_a}{\partial x^2} - U \frac{\partial c_a}{\partial x} + Ka(c_d - c_a) \qquad (4\text{-}10)$$

$$\frac{\partial c_d}{\partial t} = Kd(c_a - c_d) \qquad (4\text{-}11)$$

Laplace transformation with respect to time gives

$$D_a \frac{\partial^2 C_a}{\partial x^2} - U \frac{\partial C_a}{\partial x} - (Ka + s)\ C_a + Ka\ C_d = -\alpha_o (M/A_a)\delta(x) \qquad (5\text{-}37)$$

$$C_d = \psi C_a + (\beta_o/Kd)(M/A_d)\psi\delta(x) \qquad (5\text{-}38)$$

where ψ is defined by Equation 5-29. Elimination of C_d gives

$$D_a \frac{\partial^2 C_a}{\partial x^2} - U \frac{\partial C_a}{\partial x} - (1 + (A_d/A_a)\psi)s\, C_a = - (M/A_a)(\alpha_o + \beta_o \psi)\delta(x) \qquad (5\text{-}39)$$

Laplace transformation with respect to x gives

$$\bar{C} = \frac{(M/A_a)(\alpha_o + \beta_o \psi)}{D_a p^2 - Up - (1+(A_d/A_a)\psi)s} \qquad (5\text{-}40)$$

Inversion with respect to p and application of the boundary condition gives

$$C_a = \frac{(M/A_a)(\alpha_o + \beta_o \psi)}{\sqrt{U^2 - 4D_a(1 + (A_d/A_a)\psi)s}} \exp\left[\left(U - \sqrt{U^2 + 4D_a(1+(A_d/A_a)\psi)s}\right)\frac{x}{2D_a}\right] \qquad (5\text{-}41)$$

Using the relations developed in Equations 5-9 through 5-29, Equation 5-41 can be written at x = L as

$$C_{al} = (M/A_a U)(\alpha_o + \beta_o \psi) \frac{G}{\sqrt{1 + 2T(\alpha + \beta\psi)S}} \qquad (5\text{-}42)$$

If the measurement at x = L is made in both the main stream and the dead zone, Equation 5-32 can be combined with Equation 5-42 to give

$$C_{m1} = (M/A_a U)(\alpha_o + \beta_o \psi)(\alpha_1 + \beta_1 \psi) \frac{G}{\sqrt{1 + 2T(\alpha + \beta \psi)S}} \tag{5-43}$$

Equation 5-43 is the general transformed solution for a rapid injection made at x = 0 and the concentration measured at x = L. The factor $M/A_a U$ can be found directly from the ratio of the mass injected to the volumetric flow rate or (more commonly) indirectly from the area under the concentration-time curve.

The extension of Equation 5-43 to arbitrary injection rates instead of a rapid injection is straightforward. If material is injected at a rate $r_o(t)$ then the solution is

$$C_{m1} = (R_o/A_a U)(\alpha_o + \beta_o \psi)(\alpha_1 + \beta_1 \psi) \frac{G}{\sqrt{1 + 2T(\alpha + \beta \psi)S}} \tag{5-44}$$

where R_o is the Laplace transform of $r_o(t)$.

Inversion

The inversion of Equations 5-44 and 5-33 will now be considered. The complex inversion integral can be written

$$c(t) = \frac{1}{2\pi j} \int_{\sigma-j\infty}^{\sigma+j\infty} C(s)\ e^{st}\ ds \qquad (5\text{-}45)$$

The restrictions imposed by the boundary conditions in all transformed solutions so far considered, allow the Bromwich contour to be selected at $\sigma = 0$. Thus, s only takes on imaginary values and the complex integration can be written

$$c(t) = \frac{1}{2\pi j} \int_{-j\infty}^{+j\infty} C(s)\ e^{st}\ ds \qquad (5\text{-}46)$$

In theory, any of the transformed solutions could be inserted into the above equation and c(t) found by standard complex integration methods (6). However, in practice, quite complicated real integrals result and one is forced to simply indicate the solution in terms of these integrals. Further complicating the process is the fact that each of these integrals may present its own special numerical evaluation difficulties. As a result of these considerations it becomes advantageous to express Equation 5-46 as a real integral.

$$c(t) = \frac{1}{2\pi} \int_{-\infty}^{\infty} C(j\omega)\ e^{j\omega t}\ d\omega \qquad (5\text{-}47)$$

This form is the Fourier inversion integral which can be simplified for real functions that are zero for negative time to give

$$c(t) = \frac{1}{\pi} \int_{0}^{\infty} C(j\omega)\ e^{j\omega t}\ d\omega \qquad (5\text{-}48)$$

Numerical evaluation techniques for this integral are well developed (8,14). Appendix A describes the techniques of using Equation 5-48 to eavluate c(t).

Solutions for Diffusive Dead Zone Models

The solution of the dead zone model with diffusion into a rectangular dead zone proceeds in much the same way as the perfectly mixed case. The initial and boundary conditions for concentrations measured in the main stream at x = 0 and x = L are

I.C. $t = 0$ $\quad c_a(x,0) = 0$

$\qquad\qquad\qquad\quad c_d(x,0) = 0 \qquad (5\text{-}49)$

B.C. $x = 0$ $\quad c_a(0,t) = c_{ao}(t)$

$x = \infty$ $\quad c_a(x,t) = \text{Finite}$

$y = 0$ $\quad \dfrac{\partial c_d(0,t)}{\partial y} = 0$

$y = L_d$ $\quad c_d(L_d,t) = c_a(x,t)$ (5-50)

Equations 4-14 and 4-15 are reproduced here.

$$\frac{\partial c_a}{\partial t} = D_a \frac{\partial^2 c_a}{\partial x^2} - U \frac{\partial c_a}{\partial x} - a D_d \left.\frac{\partial c_d}{\partial y}\right|_{y=L_d} \tag{4-14}$$

$$\frac{\partial c_d}{\partial t} = D_d \frac{\partial^2 c_d}{\partial y^2} \tag{4-15}$$

Laplace transformation yields

$$D_a \frac{\partial^2 C_a}{\partial x^2} - U \frac{\partial C_a}{\partial x} - sC_a - a D_d \left.\frac{\partial C_d}{\partial y}\right|_{y=L_d} = 0 \tag{5-51}$$

$$D_d \frac{\partial^2 C_d}{\partial y^2} - s C_d = 0 \tag{5-52}$$

Solution of Equation 5-52 gives

$$\left.\frac{\partial C_d}{\partial y}\right|_{y=L_d} = \left[\sqrt{s/D_d}\, \tanh\left(\sqrt{s/D_d}\, L_d\right)\right] C_a \tag{5-53}$$

Elimination of $\left.\frac{\partial C_d}{\partial y}\right|_{y=L_d}$ yields

$$D_a \frac{\partial^2 C_a}{\partial x^2} - U \frac{\partial C_a}{\partial x} - \left[1 + (A_d/A_a) \frac{\tanh(\sqrt{s/D_d}\, L_d)}{\sqrt{s/D_d}\, L_d} \right] s C_a = 0 \qquad (5\text{-}54)$$

The similarity between this equation and the analogous equation for the perfectly mixed dead zone (Equation 5-5) is striking and it suggests further investigation. The average concentration in the dead zone can be found by the application of Equation 5-17 to the solution of Equation 5-52. There results

$$C_{dav} = \frac{\tanh(\sqrt{s/D_d}\, L_d)}{\sqrt{s/D_d}\, L_d} C_a = \Psi C_a \qquad (5\text{-}55)$$

where Ψ has been used again to indicate the transfer function between the average dead zone concentration and the main stream concentration. A summary of the definitions of Ψ for the various dead zone mechanismsis shown in Table 6. Comparison of this equation with Equation 5-4 shows that the analogy is now complete if one remembers that for the perfectly mixed case $C_d = C_{dav}$. The two different mass transfer mechanisms merely result in two different transfer functions

between the average concentrations within the dead zone and the main stream. Tables 4 and 5 show that all dead zone models can be described by the same equations. Only ψ, the transfer function, varies from case to case as shown in Tables 5 and 6.

In order to identify the parameters of this model with the term T_d (Equation 5-25), the average residence time of the dead zone must be found. This is best accomplished by expansion of the transfer function, Equation 5-55, in a series as shown in Tables 5 and 6. Thus,

$$T_d = -\frac{\frac{d\psi}{ds}\Big|_{s=0}}{\psi\Big|_{s=0}} = L_d^2/3D_d \qquad (5\text{-}56)$$

and

$$T_d = (L_d^2/3D_d)/T \qquad (5\text{-}57)$$

Therefore, ψ can be written

$$\psi = \frac{\tanh\sqrt{3T_d\, s}}{\sqrt{3T_d\, s}} \qquad (5\text{-}58)$$

With this definition of ψ the transformed solution is the same as that given by Equation 5-33 for the perfectly

mixed model. The same analogy holds true for the solution for a rapid injection and Equation 5-43 is applicable.

The measured input and rapid injection solutions for the cylindrical and spherical geometries proceed in much the same way as for the rectangular case. Both solutions result in modified Bessel functions but the spherical case can be expressed in terms of elementary functions (20).

Dead Zone Solution Characteristics

The solutions for all boundary conditions and all dead zone models are summarized in Tables 6 through 9. Tables 5 and 6 are of particular interest. They show the series expansion used to obtain the first moments or average residence times of the dead zones. All first moments have been made equal by regrouping the parameters, but the second moments, representing the variance of the residence time curves, differ. Inspection of the expansion shows that the variance increases as the dead zone model complexity increases from perfectly mixed, to rectangular, to cylindrical, to spherical. In other words, the more complex lines of mass flow associated with the more complex geometry cause a greater spread in the retention time of a particle, even though the average retention time remains the same.

Reduction to the Dispersed Flow Model

The solutions given in Table 7 reduce to the solution of the dispersed flow model, Equation 3-2, as special cases. For example, if $\beta = 0.0$, representing zero dead zone volume, the solutions for a measured input and a rapid injection shown in Table 7 become

$$\frac{C_{ml}}{C_{mo}} = \exp\left[\left(1 - \sqrt{1 + 2T}S\right)/T \right] \qquad (5\text{-}59)$$

and

$$\frac{C_{ml}}{R_o/AU} = \frac{\exp[(1 - \sqrt{1 + 2TS})/T]}{\sqrt{1 + 2TS}} \qquad (5\text{-}60)$$

As the average residence time of the dead zone approaches zero, representing an infinite mass transfer rate, the concentration in the dead zone cross section becomes equal to the main stream concentration, and the solutions again reduce to the dispersed flow solution. This is most easily seen by letting $T_d = 0.0$ in the series expansion in Table 5 and noting that $\psi = 1.0$ for all cases. Thus, the solutions shown in Table 7 again reduce to Equations 5-59 and 5-60. Also, as the average residence time of the dead zone becomes

infinite, representing a zero mass transfer rate, the dead zone is isolated, and reduction to the dispersed flow model again occurs since $\psi = 0.0$ for all cases. Now, however, the average residence time of the system has been reduced by a fraction β, representing the fraction of the volume deleted. The resulting equations are

$$\frac{C_{ml}}{C_{mo}} = \exp\left[\left(1 - \sqrt{1 + 2T(\alpha T)\, s}\right)/T\right] \tag{5-61}$$

and

$$\frac{C_{ml}}{R_o/AU} = \frac{\exp\left[\left(1 - \sqrt{1 + 2T(\alpha T)\, s}\right)/T\right]}{\sqrt{1 + 2T(\alpha T)\, s}} \tag{5-62}$$

If $T = 0.0$, representing no dispersion transport in the main stream, the solutions shown in Table 7 become respectively

$$\frac{C_{ml}}{C_{mo}} = \frac{\alpha_1 + \beta_1 \psi}{\alpha_o + \beta_o \psi} \exp\left[-(\alpha + \beta\psi)\, S\right] \tag{5-63}$$

and

$$\frac{C_{ml}}{R_o/AU} = (\alpha_o + \beta_o \psi)(\alpha_1 + \beta_1 \psi) \exp\left[-(\alpha + \beta\psi)\, S\right] \tag{5-64}$$

These solutions could be referred to as solutions of a plug flow dead zone model. For $\beta = 1.0$ and $T = \infty$ the solutions in Table 7 have no physical meaning.

Interpretation of the Dead Zone Concentration-time Curves

Figure 4 shows typical concentration-time curves resulting from the rapid injection solution of the perfectly mixed dead zone. For the calculation of these curves it was assumed that the injection and measurement were made in the main stream. Thus, Equation 5-43 was used with $\beta_o = \beta_1 = 0.0$ and $\alpha_o = \alpha_1 = 1.0$. Numerical inversion techniques, described in Appendix A, were used to find the concentration as a function of time.

The solutions are plotted as T_d varies from zero to infinity. As was previously demonstrated, when $T_d = 0.0$, representing an infinite mass transfer rate, the solution is given by the dispersed flow model. The result is a slightly skewed Gaussian curve. As the average residence time of the dead zone is increased, the dead zone begins to pick up and retain material, resulting in attenuation of the curve peak and an increase in the tail as material is redeposited in the main stream. When $T_d = 0.2$, the dead zone mechanism completely dominates the spread of tracer,

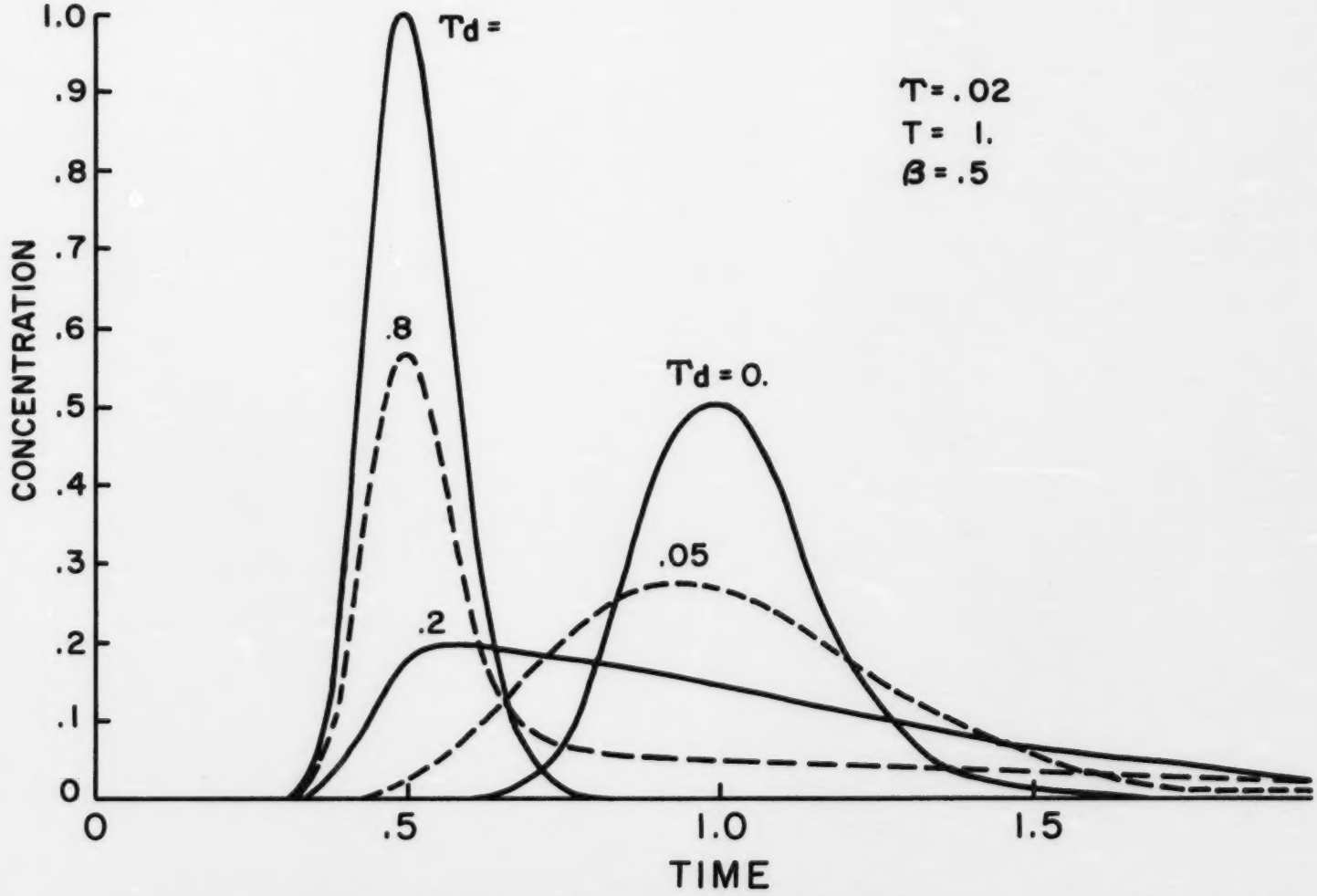

FIGURE 4 RAPID INJECTION SOLUTION OF PERFECTLY MIXED DEAD ZONE MODEL.

resulting in a long, highly skewed curve with linear decay. When the average residence time reaches $T_d = 0.8$, the mass transfer rate is so low that much of the tracer cloud flows by without being transferred to the dead zone. As a result, the initial portion of the curve is similar to the dispersed flow solution but the material re-enters the main stream so slowly that a very long, slowly decaying tail is produced. The length of this tail is indicated by its effect upon the first moment, which is $T = 1.0$ for all the curves (except $T_d = \infty$). As T_d approaches infinity the solution again reduces to the dispersed flow solution, but now the dead zone has been isolated from the main stream and the average residence time is $T = 0.5$. Thus, the first moment or average residence time changes discontinuously from $T = 1.0$ to $T = 0.5$ as T_d approaches infinity.

In Figure 4 the values of the relative dispersion coefficient and the dead zone fraction were $T = .02$ and $\beta = 0.5$. The shapes of the curves for other values of these parameters are easily visualized. For example, when β is decreased toward zero, the position of the curve shifts to the right and its peak decreases. The shapes of the other curves are of the same form, but peak truncation and spread

are reduced. When $\beta = 0.0$ all curves reduce to the $T_d = 0.0$ curve. If β is increased, just the opposite effect takes place. The $T_d = \infty$ curve moves further to the left and the attenuation and spread of the other curves become more severe.

The effect of variation in the relative dispersion coefficient, T, is more pronounced on the $T_d = 0$ and $T_d = \infty$ curves. Decreasing the value of T will make these curves more peaked and will affect other curves in the same way but to a lesser degree. Increasing the value of T will have the opposite effect.

Moments

Although the determination of parameters from moments calculated from experimental data can lead to serious errors, it is instructive to note the theoretical effect of the dead zones on the first three moments of the solutions (14,26). Only the moments of G, defined by Equation 5-27, will be considered as all other quantities in the solutions arise as a result of boundary conditions. The first three moments of G are found utilizing methods outlined by Leonard and Ruszkoy (16).

1st MOMENT ABOUT ORIGIN $\quad T \quad$ (5-65)

2nd MOMENT ABOUT MEAN $\quad T^2 (T + 2\beta T_d) \quad$ (5-66)

3rd MOMENT ABOUT MEAN $3T^3(T^2 + T\beta T_d + 2\gamma\beta T_d^2)$ (5-67)

where γ is the second coefficient in the series expansion shown in Table 6. One of the advantages of the parameters grouping is now evident, since the average residence time is simply T and all the other groups appear as multiplicative factors. The variance or second moment shows the kind of dependence on T, β, and T_d that might have been expected. Increasing the relative dispersion coefficient, or the dead zone fraction, or the dead zone residence time, all increase the second moment.

The third moment is perhaps the most informative. The strong positive dependence upon T_d clearly illustrates that the dead zone models can exhibit the marked skewness observed in much experimental data. It can also be seen that the first and second moments can be held constant by holding T, T and βT_d constant, while the third moment can be varied to produce the desired degree of skewness by varying the individual values of β and T_d.

From these moment considerations and the shapes of the curves in Figure 13 it can be concluded that the dead zone models show promise as a mechanism to explain mass

transport in streams and rivers. However, mild dependence of the third moment upon γ, and the fact that this parameter need not be used to adjust the first three moments, indicate that the geometrical form of the dead zone may not be too important.

CHAPTER VI

CHANNEL EXPERIMENTS

In order to test the concepts of the dead zone model under controlled conditions, a series of tracer experiments was performed in a rectangular laboratory channel. The channel was about sixty feet long, two feet wide, and one foot deep. It had provisions for varying the slope, flow rate, and depth of the recirculated water. The sides of the channel were made of glass and the bottom was painted with an electrically nonconductive epoxy paint. Various nonconductive screens for artificially roughening the channel bottom were available.

Equipment was designed to inject rapidly a line source upon the surface of the water. This was accomplished by using a section of ¼-inch copper tubing bent into a rectangular hoop as shown in Figure 5. The tubing had a series of small holes bored on the underside and was connected through a solenoid valve to a pressurized tank of NaCl solution. Injections were accomplished by operating the solenoid valve with a timer. A drip pan was constructed to insure against leakage between injections. All injections were made across

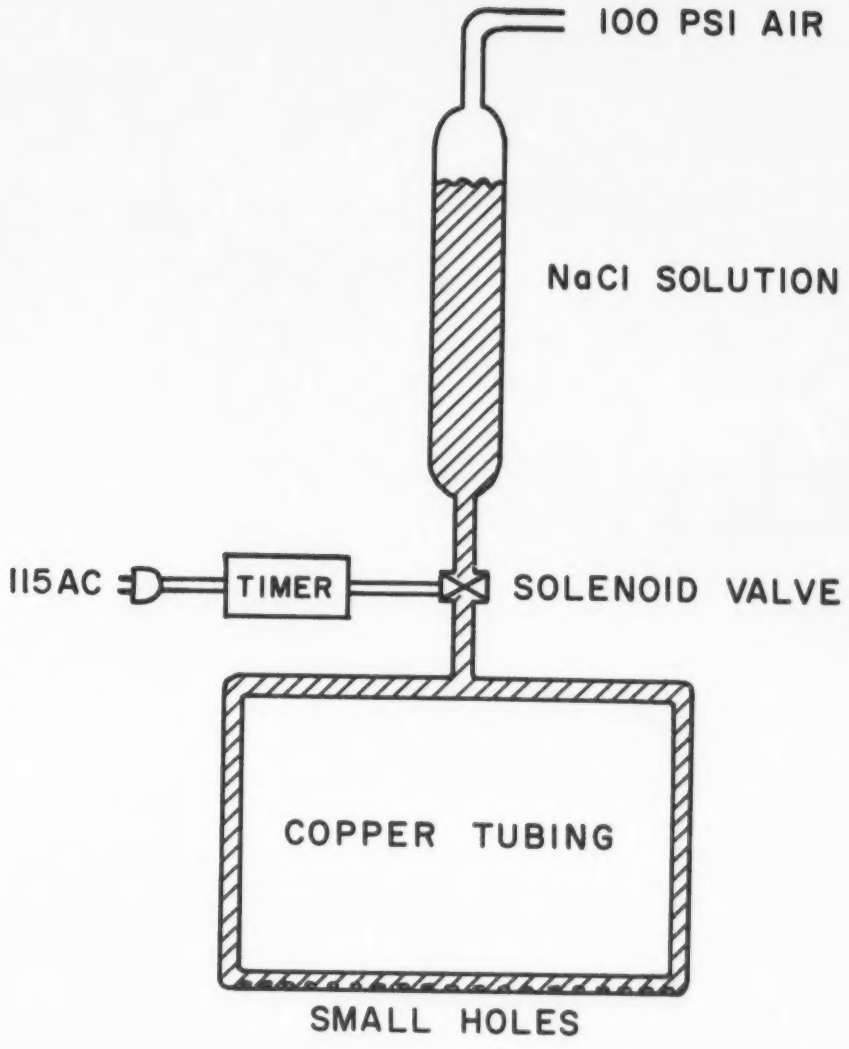

FIGURE 5 INJECTION APPARATUS

the entire width of the channel.

Preliminary experiments were conducted to visualize how rapidly vertical uniformity was achieved. A small quantity of dye was added to the NaCl solution. It was observed that vertical mixing was essentially complete within one or two feet if a saturated solution of NaCl was used. The higher density of the saturated solution seemed to aid the initial mixing. After initial mixing, vertical uniformity of the dye indicated the density difference between the tracer cloud and the water was negligible.

The cross-sectional average concentration was measured at a point forty feet downstream by the use of specially constructed conductivity probes. Initial design attempts failed due to small surface waves which caused a varying path length between conductivity probes. This effect produced an unacceptable noise level and destroyed much of the available information in the concentration-time records.

In the final design of the conductivity probes, the surface effect was eliminated by placing a piece of ¼-inch plexiglass tangent to the water surface. The plexiglass, shown in Figure 6 , was one foot long with flared ends and

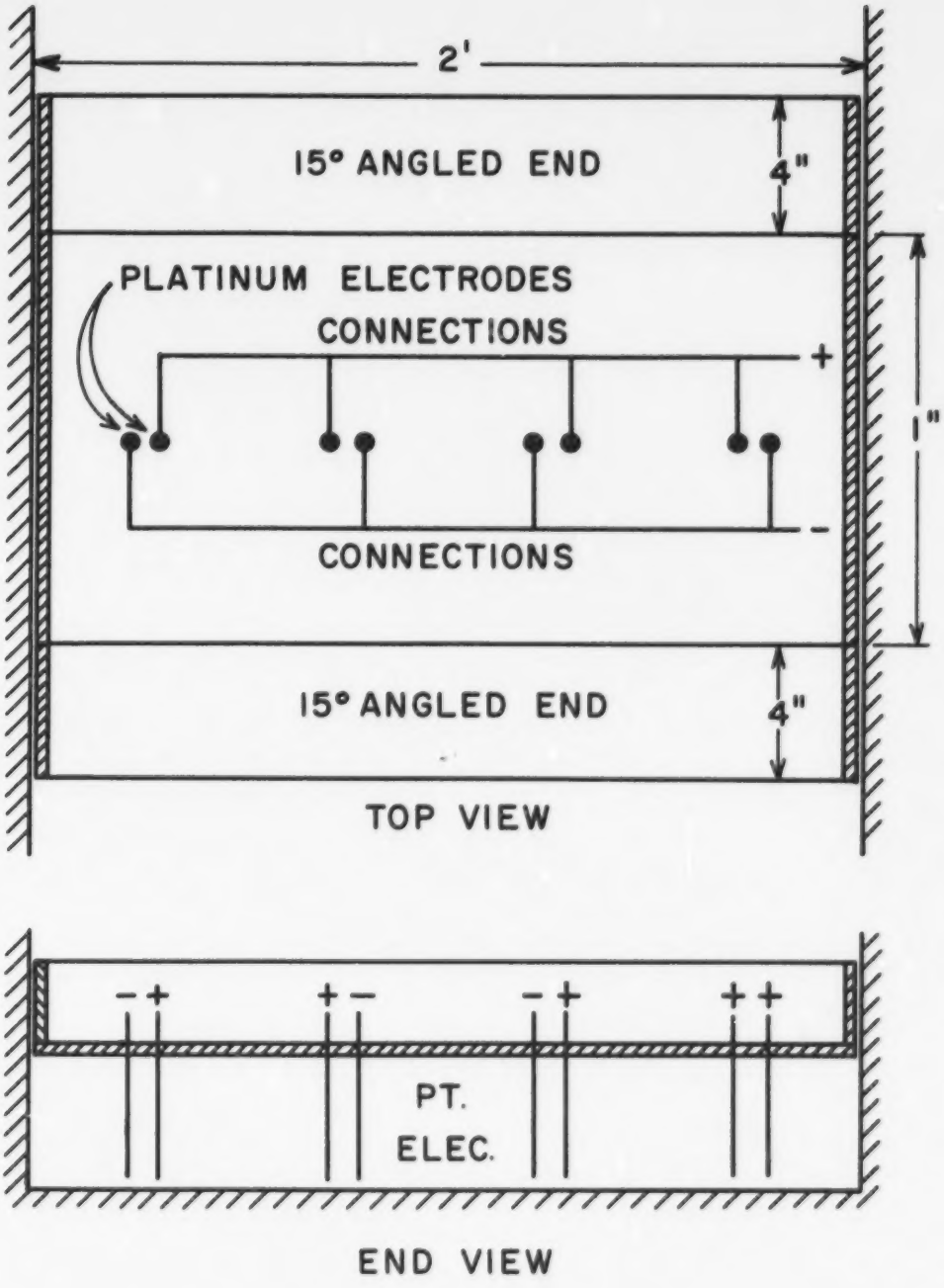

FIGURE 6 CONDUCTIVITY PROBES

about 1/16 inch narrower than the width of the channel. The sides were boxed in to prevent water from spilling over the top of the plexiglass. Four sets of platinum wires were inserted into close fitting holes bored vertically along the centerline of the plexiglass. The platinum wires extended beyond the bottom of the plexiglass a distance slightly less than the depth of the water being tested. There was a one-inch spacing between probes. The four probe sets were equally spaced laterally in order to obtain the most uniform lateral averaging, and they were connected in parallel in order to achieve correct averaging. The polarity of the connections, shown in Figure 6, was designed to minimize interaction between probe sets. A platinum black coating was electroplated on the electrodes by standard methods (7).

A Sanborn model 64-1300 strip chart recorder with strain gauge bridges was used to record the concentration-time curves as measured by the conductivity probes. An impedance substitution box was used for the matching arm of the bridge, since baseline drift, due to change in physical properties, was negligible. The recorder had an event marker which was activated by the injection timer, thus accurately fixing the time of injection on the chart.

The channel experiments were not designed to simulate, on a model basis, the phenomena observed in real streams. The difficulties and limitations of this approach are discussed at some length in Appendix B. These experiments were conducted only to test, under controlled conditions, the acceptability of the physical and mathematical concepts of the dead zone model.

Various schemes were attempted to create dead volumes and mass transfer rates that could be systematically varied from run to run. The most successful method was to line one or both sides of the channel with bricks. Varying the number and arrangement of the bricks produced a wide variation in the dead zone volume and the mass transfer rate.

Three basic brick patterns were used as shown in Figure 7. The bricks were spaced uniformly throughout the forty-foot test section. The number of bricks, using these basic patterns, was varied from one to forty-two. A total of one hundred and fifty-seven runs were made using one to three duplications for each configuration, although more duplications were made on some configurations. About twenty runs were made with forty to forty-two bricks in special configurations, arranged to extend the range of the dead

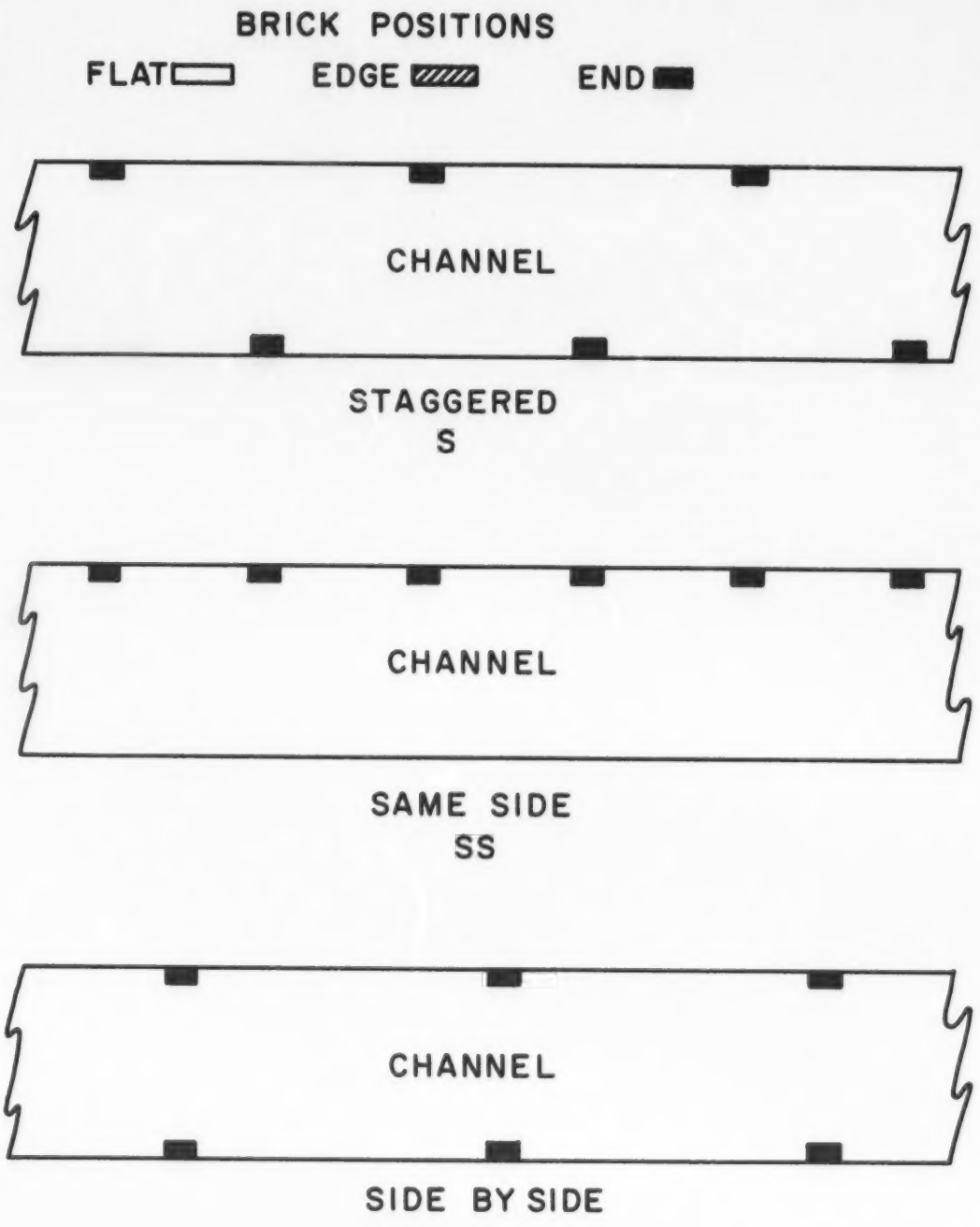

FIGURE 7 STANDARD BRICK ARRANGEMENTS

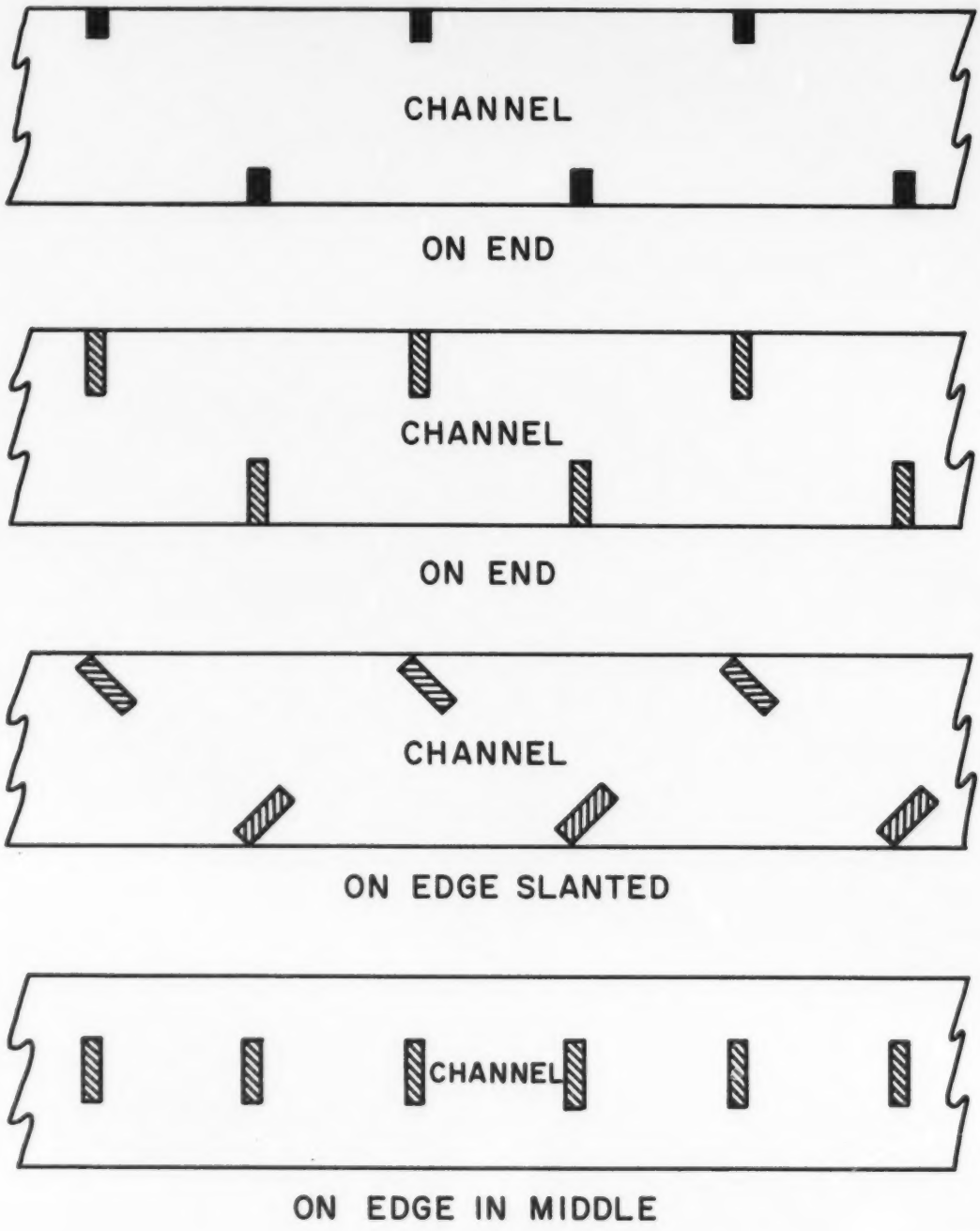

FIGURE 8 SPECIAL BRICK ARRANGEMENTS

zone fraction and mass transfer rate. Typical configurations for these runs are shown in Figure 8.

The observed experimental results were compared to the results predicted by the dead zone and dispersed flow models. The appropriate solution for the dispersed flow model is Equation 5-60, and for the dead zone model, Equation 5-43 with $\alpha_o = \alpha_1 = \alpha$ and $\beta_o = \beta_1 = \beta$, was used. The parameters for the models were found by a least squares procedure described in Appendix A. As was anticipated in the previous section from moment considerations, there was no significant difference in the ability of the various dead zone models to predict the observed results. The difference between the observed and predicted concentration-time curves was of the order of magnitude of the experimental error for all dead zone models. For larger dead zone fractions and smaller mass transfer rates, the diffusional models were slightly better than the perfectly mixed model, but the difference was not considered significant. Table 10 shows the results of the model fits for three typical cases. The parameters were not calculated for the cylindrical model but the series expansions for ψ (Table 5) indicate these values should be somewhere between the values for the rectangular and spherical diffusion dead zone models.

TABLE 10

TYPICAL COMPARISONS OF MODEL PARAMETERS:

CHANNEL EXPERIMENTS

RUN IDENTIFICATION: H18B

BRICK ARRANGEMENT: 3 BRICKS STAGGERED

MODEL	T	T	β	T_d	SE
DISPERSED FLOW	0.01653	34.8			0.034
PERFECTLY MIXED DEAD ZONE	0.00699	35.6	0.121	0.048	0.013
RECTANGULAR DIFFUSION D.Z.	0.00689	33.1	0.077	0.023	0.013
SPHERICAL DIFFUSION D.Z.	0.00687	33.1	0.065	0.020	0.013

RUN IDENTIFICATION: H160B

BRICK ARRANGEMENT: 34 BRICKS SIDE BY SIDE

MODEL	T	T	β	T_d	SE
DISPERSED FLOW	0.04854	35.1			0.099
PERFECTLY MIXED DEAD ZONE	0.01036	41.0	0.228	0.212	0.012
RECTANGULAR DIFFUSION D.Z.	0.00806	35.7	0.170	0.113	0.011
SPHERICAL DIFFUSION D.Z.	0.00793	35.1	0.153	0.101	0.011

RUN IDENTIFICATION: H75AD

BRICK ARRANGEMENT: 12 BRICKS SAME SIDE

MODEL	T	T	β	T_d	SE
DISPERSED FLOW	0.01709	31.5			0.080
PERFECTLY MIXED DEAD ZONE	0.00800	33.7	0.100	0.147	0.025
RECTANGULAR DIFFUSION D.Z.	0.00862	32.4	0.077	0.127	0.023
SPHERICAL DIFFUSION D.Z.	0.00808	32.4	0.074	0.122	0.022

There was, however, a marked difference in the predictive ability of the dispersed flow and dead zone models. Appendix C is a tabulation of the parameters and standard errors of estimate for the dispersed flow model and the perfectly mixed dead zone model. The standard errors of estimate are normalized values and may be looked upon as average percentage errors. The ratio of the squared deviations of the dispersed flow model to the squared deviations of the dead zone model are listed as the F statistic. Ninety-five percent confidence limits were used to indicate that 95% of the F values above 1.85 are due to the superior predictive ability of the dead zone model and only 5% are due to chance. Figures 9 , 10, and 11 are bar graphs of the F values. All values above the F = 1.85 horizontal line indicate a superior predictive ability for the dead zone model.

Figure 12 shows a typical concentration-time experimental curve as well as the least squares best predictions for the dispersed flow and dead zone models. It can be seen that the dispersed flow model is not at all representative of the observed results. On the other hand the dead zone model is identical with the observed data within the limits of experimental errors.

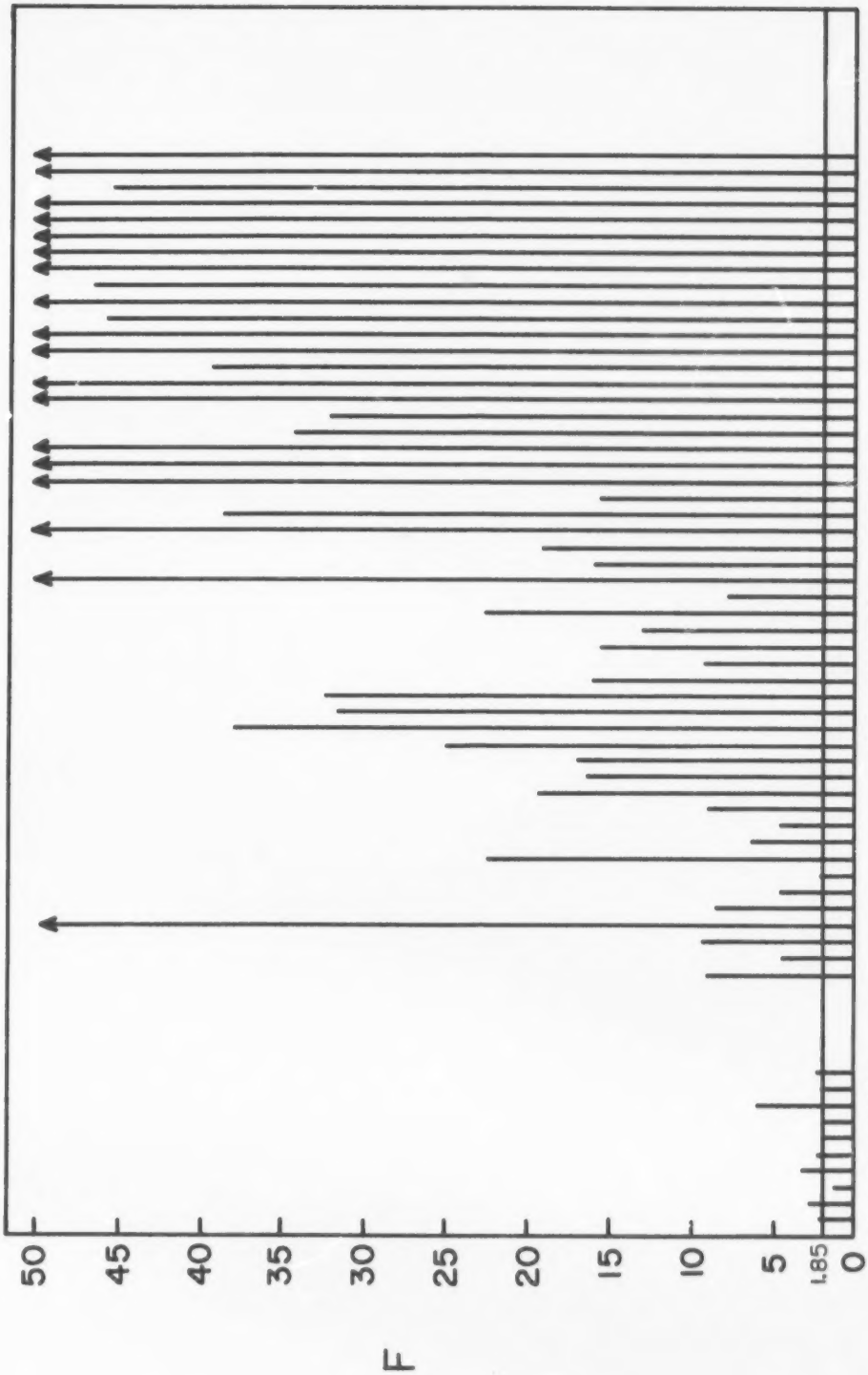

FIGURE 9 F STATISTIC FOR CHANNEL TESTS

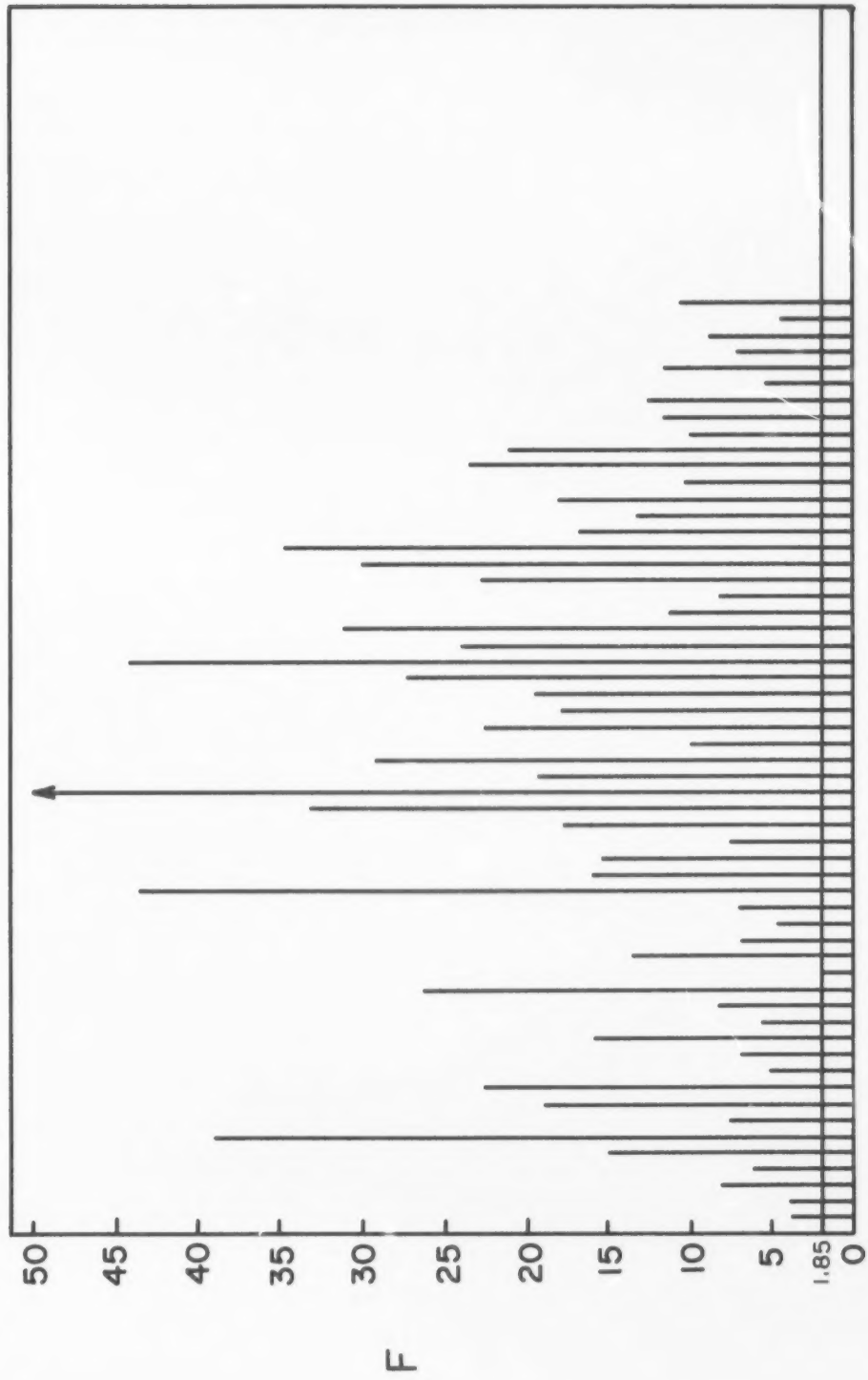

FIGURE 10 F STATISTIC FOR CHANNEL TESTS

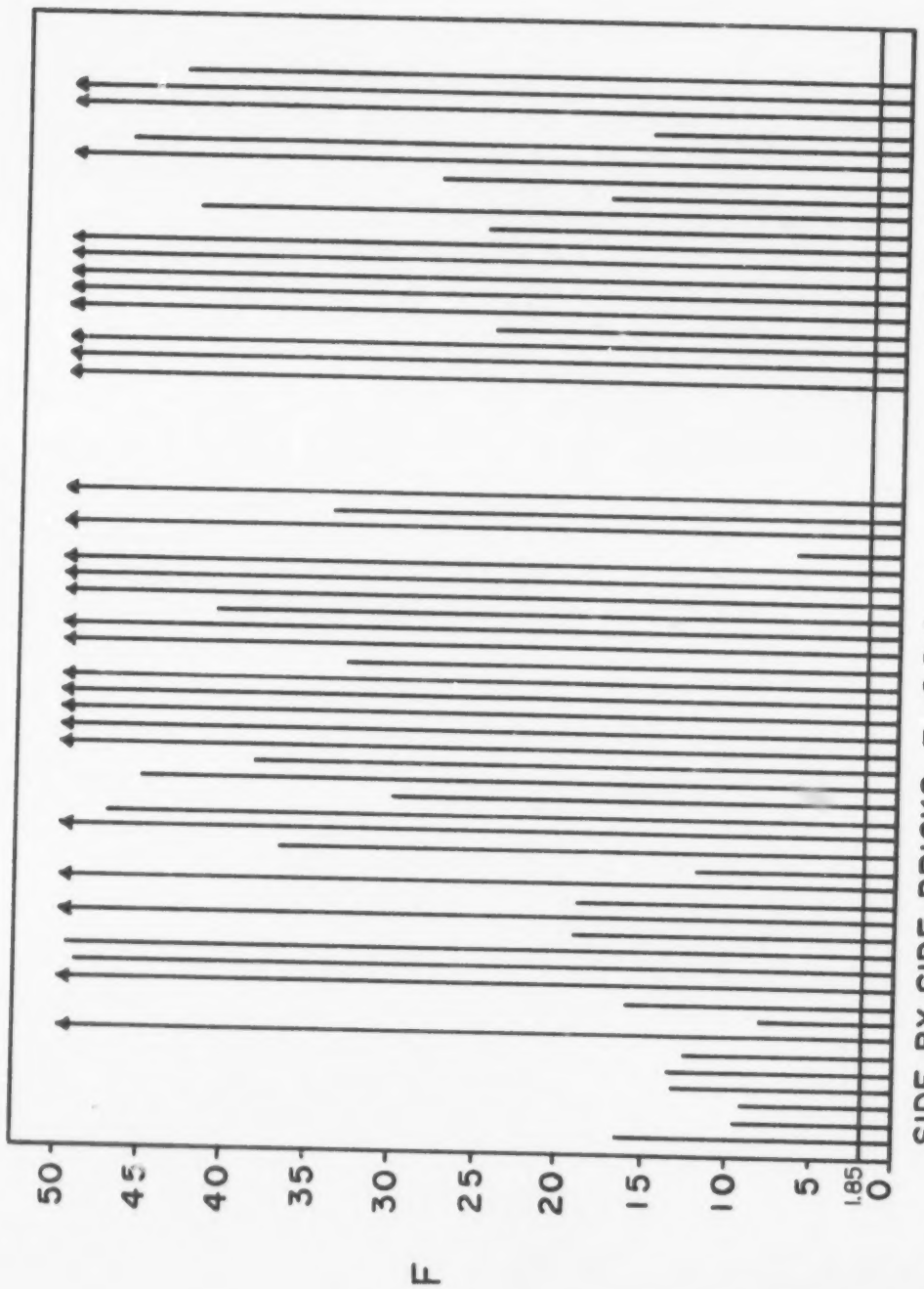

FIGURE 11 F STATISTIC FOR CHANNEL TESTS

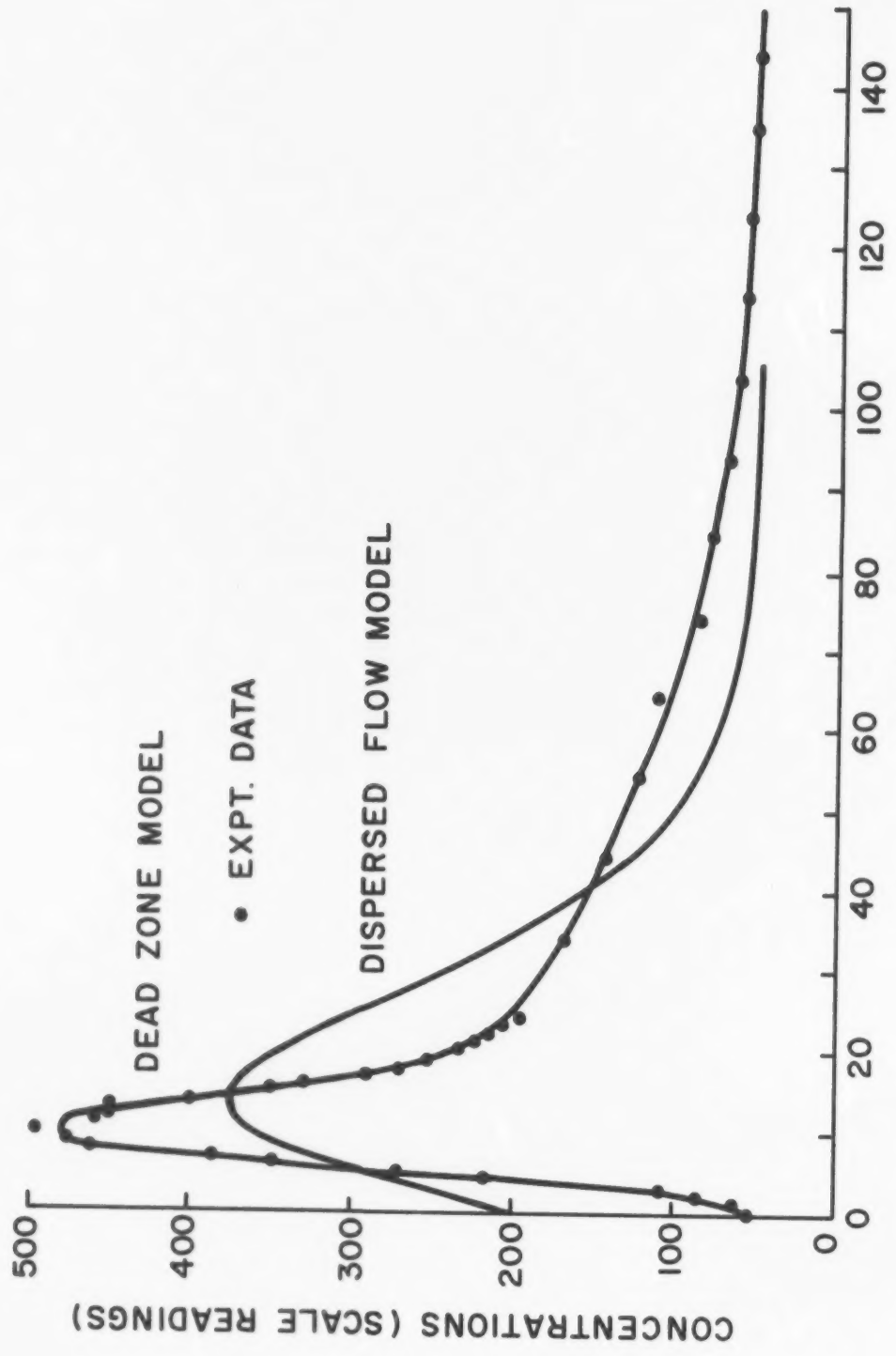

FIGURE 12 DISPERSED FLOW AND DEAD ZONE MODEL FITS.

It was concluded from the channel tests that the dead zone concept is a satisfactory representation of mass transport in situations where relatively stagnant volumes are present. The inadequacy of the dispersed flow model in such situations was also clearly illustrated.

CHAPTER VII

RIVER EXPERIMENTS

A number of factors had to be considered in the selection of streams and rivers for tracer experiments. It would be desirable to test an "average" stream in order to make an unbiased comparison of the predictive abilities of the dispersed flow and dead zone models. This "average" stream is difficult to describe except in general terms: It should have some bank unevenness, stagnant regions, and debris, but not too much. It should have some non-uniformity in depth, width, and cross-sectional area, but not too much. It should have an "average" lateral velocity gradient. Fortunately, however, the rivers and reaches had already been selected to satisfy other objectives of the testing program and the "average" river did not have to be found (26).

The rivers and reaches were selected primarily to satisfy the requirements of a program designed to investigate the correlation of oxygen uptake and the dispersion coefficient (26). These selections emphasized uniformity, lack of stagnant regions and debris along the banks, etc.

Thus, many factors explained by the dead zone model were absent and the results must be considered biased in favor of the dispersed flow model. This arrangement was felt to be satisfactory since it would more strongly emphasize the superiority of the dead zone model.

Reaches on the Clinch, Hiwassee and French Broad Rivers were tested. Complete details as to the location, depth, width, flow rate, etc., can be found in references 5 and 26. Rhodamine-B dye was used as the conservative tracer. The advantages of fluorometric tagging have been adequately discussed in the literature, and it suffices to say here that it was found to be an ideal tracer.

The testing procedure was again designed for the introduction of a line source on the surface of the river. In the channel experiments it was possible to measure the cross-sectional average concentration, including both the main stream and the dead zone. However, due to limitations in equipment and personnel it was not possible to design a measurement scheme to measure the cross-sectional average concentration in a river. Thus, it was decided to make the line injection in the main stream only, and to consider a single concentration measurement made in the main stream

as representative of the main stream concentration. Such a testing procedure further biased the experiments in favor of the dispersed flow model since the effects of dead zones are further diminished by such an injection.

The injection of the line source was accomplished by dumping from a boat, a quantity of Rhodamine-B diluted to facilitate even lateral distribution. The boat path was adjusted for current drift during injection so as to best approximate a line source. The injection was made only into the main stream. It was not very difficult to determine the main stream boundaries as a trial injection readily showed the sharp velocity gradient marking the transition from the main stream to the dead zone.

In the experiments on the Clinch and French Broad Rivers the concentration-time curves were obtained by grab sampling from a boat located at a representative point in the main stream. Samples were taken at intervals from ten seconds to five minutes, depending upon the rapidity with which the concentration was changing. It was easy to see the tracer cloud pass as the injected quantity was adjusted to give peak concentrations of about one hundred parts per billion. This peak value was about ten times the recommended

peak for Rhodamine-B dye testing, but in addition to visual observation advantages, it improved the signal to noise ratio. The grab samples were analyzed on a Beckman model 772 fluorometer.

The tests on the Hiwassee River were all made using an American Instrument model 10-213 flow-through fluorometer. A 115V A.C. Cornell-Dubilier "Powercon" inverter operated by a 12V battery was used as the power supply for the fluorometer and a strip chart recorder. A battery operated centrifugal pump was used to pump the sample stream through the fluorometer. Data collection using the flow-through fluorometer was superior in every respect to grab sampling.

Forty-one runs were made on the Clinch, French Broad, and Hiwassee Rivers. Again the least squares best parameters were found according to techniques described in Appendix A. Only the perfectly mixed dead zone model and dispersed flow model were considered. A tabular summary of the results can be found in Appendix D. The lack of debris, stagnant regions, and bank unevenness is reflected in the small dead zone percentage. Most values of β were less than five percent. In spite of the small dead zone percentages and other unfavorable factors previously mentioned, the F statistic shows the

dead zone model superior to the dispersed flow model in thirty-five out of forty-one cases. Figure 13 is a bar graph of F values.

It was desired to strengthen the conclusion of superiority of the dead zone model by the use of the results of tracer experiments published in the literature. Although many such references can be found, it seems that most were carried out for special purposes, such as, the determination of flow rate, determination of peak concentrations, etc.

However, one study, by Godfrey and Fredrick (12), was well suited for analysis, since it was made for the purpose of studying dispersion in natural streams. After correcting the data for decay of the radioactive tracer, a least squares best fit of the dispersed flow model was accomplished for all runs. Again methods described in Appendix A were used. The deviations of the predicted curves from the observed curves were similar for all runs and are well illustrated by Figure 1.

Least squares best fits of the perfectly mixed dead zone model on a representative number of the runs all produced the same results. The dead zone model predictions were all superior to the dispersed flow predictions and generally the predictions were the same as the observed values within the limits of experimental error.

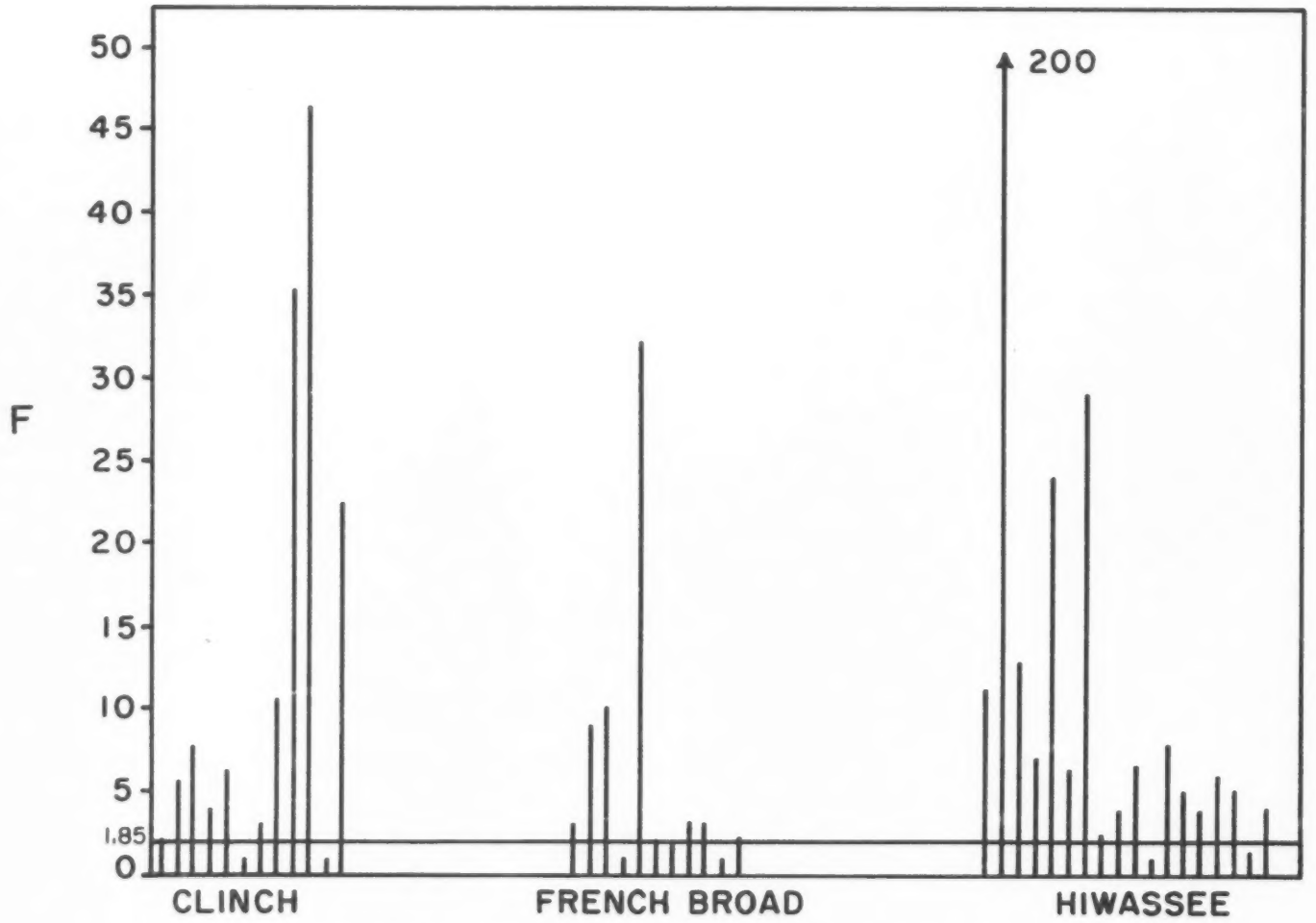

FIGURE 13 F STATISTIC FOR RIVER TESTS

CHAPTER VIII

CONCLUSIONS

The description of the transport of an inert tracer by streams and rivers is important as the basis of many studies involving the interaction of pollutants with the fresh water environment. The dispersed flow description suffers a deficiency that appears symptomatically as an inability to describe certain skew and tailing characteristics of the concentration-time curves. This deficiency can be attributed to the wide variation in hydraulic conditions within the cross section of a stream or river which produces stagnant regions along the banks and bottoms of the streams and rivers.

The dead zone model is a more realistic description than the dispersed flow model since it describes separately the two dominant transport regions: the main stream and the stagnant or dead zone. These two regions are physically connected by a mass transfer mechanism which results in two coupled partial differential equations as the mathematical model.

A comparison of the ability of the dispersed flow and dead zone models to describe the spread of inert tracer in both channels and river experiments clearly demonstrated the superiority of the dead zone model. The dead zone model was generally able to describe the spread of tracer within the limits of accuracy of the experimental data.

The dead zone model incorporates two more parameters than the dispersed flow model: β and T_d. The disadvantages of these two extra degrees of freedom are offset by the physical significance that can be attached to β and T_d. The value of the dead zone model is further enhanced by giving a definite physical meaning to the relative dispersion coefficient, T, and by absorbing the other degree of freedom into a parameter, T, associated with only the system size and flow rate.

The prediction of numerical values of the dead zone parameters from such hydraulic and geometric parameters as the slope of the energy grade line, the stream depth, width, and flow rate, etc., would certainly enhance its usefulness. Unfortunately, this does not seem possible. The values of the dead zone parameters are affected by many factors that are not measured by the usual stream parameters. For

example, the velocity profile, bank and bottom unevenness, debris along the banks, cross-sectional nonuniformity, etc., are not directly associated with the usual hydraulic and geometric parameters. This poor correlation of the model parameters with the usual stream parameters is not unique to the dead zone model. It plagues all descriptions and it is the direct result of the diversity and complexity of the hydraulic conditions that exist in streams and rivers.

As a result of the above considerations it seems that the most appropriate way to obtain model parameters for a given stream or river is to perform tracer tests. Certainly, this is a more straightforward and less expensive approach than trying to measure in intricate detail all the factors that affect the model parameters.

However, in spite of all the difficulties, some progress has been made in finding a correlation that will give a rough estimate of the value of the relative mixing coefficient, T. In a thesis concurrent to this work, Thackston (26) has shown the following expression to be useful in estimating T.

$$T = 11.64 \frac{h}{L} \left[\frac{U_*}{U}\right]^{3/4} \qquad (8\text{-}1)$$

where h is the mean stream depth and U_* is given by the following equation

$$U_* = (Se\ h\ g)^{\frac{1}{2}} \qquad (8\text{-}2)$$

where Se is the slope of the energy grade line. The constant 11.64 was determined from the results of the river tracer experiments listed in Appendix D. Figure 14, taken from Thackston's work with slight modifications, is a plot of Equation 8-1 solved for D and D_a. It shows the improvement in the correlation of dispersion with the hydraulic parameters when values of the dispersion coefficient are found by the use of the dead zone model rather than the dispersed flow model. Perhaps a reasonable explanation for the improved correlation is the fact that D_a is only associated with the main stream which is not directly affected by debris, sharp velocity profiles, etc. Thus, the main stream and its associated parameter may vary in a predictable manner from stream to stream.

The value of the dead zone model as a starting point for more complicated studies involving reaction, etc., will have to be judged from the results of these studies. However, some insight can be gained from an application where the dead

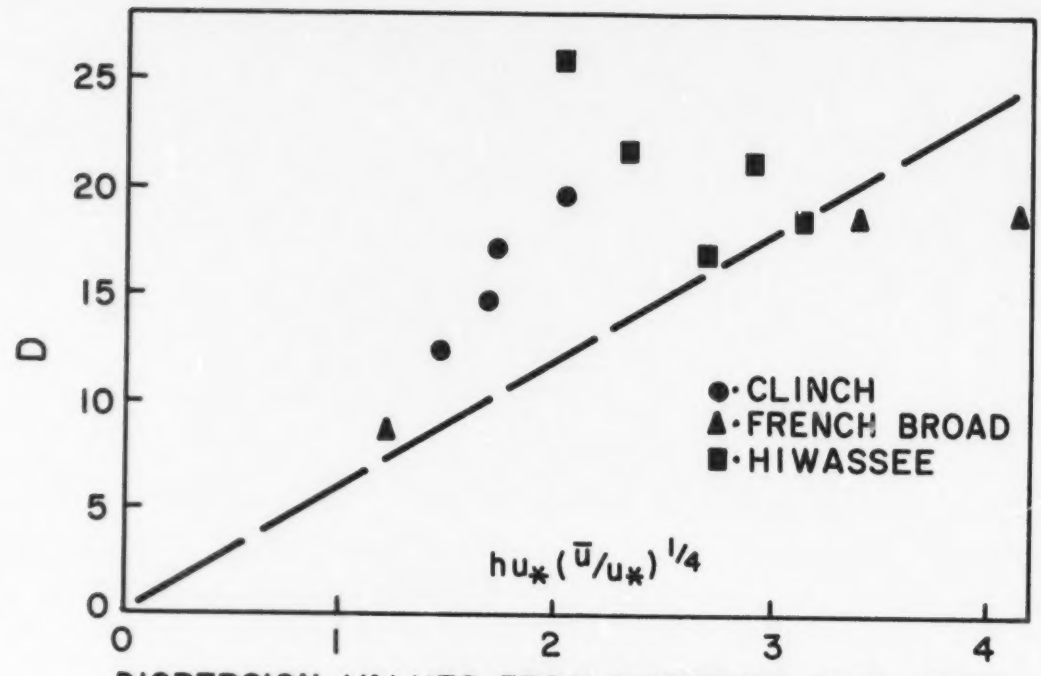

DISPERSION VALUES FROM DISPERSED FLOW MODEL

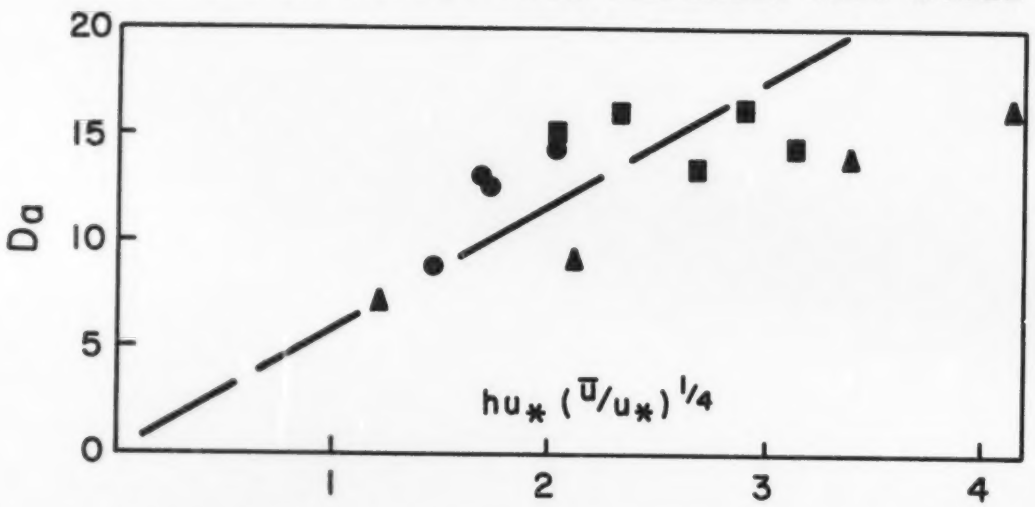

DISPERSION VALUES FROM DEAD ZONE MODEL

FIGURE 14 PREDICTION OF THE DISPERSION COEFFICIENT.

zone model has already proved its value.

A study was undertaken to determine the correlation of rate of oxygen uptake with dispersion characteristics in streams (26). It was suspected that mixing effects due to debris and stagnant regions along the bank was influencing the correlation since these effects would increase dispersion, but would have no effect upon oxygen uptake. The correlation was significantly increased when the dead zone model was used to isolate the more important effects of dispersion in the main stream.

If further applications of this nature can be found, the dead zone model may prove to be a useful tool in studies leading to the prevention of pollution, and the cleaning of polluted waters.

APPENDICES

APPENDIX A

FREQUENCY DOMAIN MODEL EVALUATION[1]

The Least Squares Criterion

Although a number of comparison criteria have been used in particular mathematical modeling applications, one of the simplest and most widely applicable criteria for dynamic systems is the integral of the squared error between the observed and predicted results. More exactly the integral should be formulated over all space and time but, for many applications, interest is directed to a particular point in space and the time varying error at this point is considered. Thus, the expression for the integral squared error at such a point is

$$\phi = \int_0^\infty [y_o(t) - y_p(t)]^2 \, dt \qquad \text{(A-1)}$$

where t is time, and $y_o(t)$ and $y_p(t)$ are, respectively, the observed and predicted responses.

Minimization of ϕ is commonly called the least squares

---

[1]Nomenclature for Appendix A is unique and is listed at the end of Appendix A.

procedure. Since the equations for the predicted response are in general nonlinear in the system parameters, an explicit least squares solution is usually not available, and the minimization of ϕ is accomplished by a regressive technique. Marquardt (17,18) has developed an effective nonlinear least squares algorithm and has successfully incorporated it into a computer program.

For certain simple models it may be satisfactory to apply the nonlinear least squares procedure directly to the expression for ϕ given by Equation A-1. However, for more complicated models, or for systems that have been excited by a measured input, it is very difficult to find and compute the predicted response, $y_p(t)$. The following sections show how this can be avoided by transformation of the least squares criterion to the frequency domain.

Fourier Transforms for Real Functions

The Fourier transform pair may be written as

$$F(j\omega) = \int_{-\infty}^{\infty} f(t)\ e^{-j\omega t}\ dt \qquad \text{(A-2)}$$

$$f(t) = \frac{1}{2\pi} \int_{-\infty}^{\infty} F(j\omega)\ e^{j\omega t}\ d\omega \qquad \text{(A-3)}$$

where $F(j\omega)$, the Fourier transform of $f(t)$, has been written as a function of $j\omega$ in recognition of its relation to the Laplace transform. If $f(t)$ is restricted to a real function equal to zero for $t < 0$, Equations A-2 and A-3 become

$$F(j\omega) = \int_0^\infty f(t)\, e^{-j\omega t}\, dt \qquad f(t) = 0,\ t < 0 \tag{A-4}$$

$$f(t) = \frac{1}{\pi} \int_0^\infty F(j\omega)\, e^{j\omega t}\, d\omega \qquad f(t) = \text{Real} \tag{A-5}$$

The reader is referred to Guillemin (13) for further information on Fourier transform theory.

Transformation of the Least Squares Criterion to the Frequency Domain

According to Parseval's theorem there is a relationship between the squared magnitudes of the Fourier transform pair.

$$\int_{-\infty}^{\infty} [f(t)]^2\, dt = \frac{1}{2\pi} \int_{-\infty}^{\infty} |F(j\omega)|^2\, d\omega \tag{A-6}$$

For real functions which are zero for negative time this becomes

$$\int_0^\infty [f(t)]^2\, dt = \frac{1}{\pi} \int_0^\infty |F(j\omega)|^2\, d\omega \tag{A-7}$$

Application of this result to the least squares criterion

given by Equation A-1 yields the frequency domain expression for ϕ.

$$\phi = \frac{1}{\pi} \int_0^\infty |Y_o(j\omega) - Y_p(j\omega)|^2 \, d\omega \qquad \text{(A-8)}$$

Equation A-8 shows that while ϕ depends upon the squared scalar deviations in the time domain, it depends upon the squared vectorial deviations in the frequency domain.

Numerical Fourier Transformation

The system response, $y_o(t)$, is measured experimentally in the time domain, and it is necessary to have a method for numerically transforming $y_o(t)$ to $Y_o(j\omega)$ in order to use Equation A-8. The problem of finding the numerical Fourier transform of a function f(t) that is given as a graph or a series of discrete points has been explored by Clements and Schnelle (9). Their approach in evaluating $F(j\omega)$ was to break the integral, given by Equation A-4, into a real and an imaginary part as shown below:

$$F(j\omega) = \int_0^\infty f(t) \cos \omega t \, dt + j \int_0^\infty f(t) \sin \omega t \, dt \qquad \text{(A-9)}$$

or

$$F(j\omega) = R(\omega) + j \, I(\omega) \qquad \text{(A-10)}$$

The integrals representing $R(\omega)$ and $I(\omega)$ were evaluated using special quadrature formulas. However, an approach that is more flexible and more efficient is available through the Laplace transform.

This method assumes that $f(t)$ can be represented by a function made up of a series of polynomial segments. Ordinary discontinuities in the function and its derivatives are allowed at the union of the segments. The time domain equation for this function is

$$f(t) = \sum_{i=1}^{n} u(t - T_i)[A_i + B_i(t - T_i) + C_i(t - T_i)^2 + D_i(t - T_i)^3 + \ldots] \tag{A-11}$$

where the jump in the function at T_i is given by A_i, the jump in the first derivative at T_i is B_i, the jump in the second derivative at T_i is C_i, etc. The notation $u(t-T_i)$ represents a unit step function and it indicates that additions to the function $f(t)$, causing the jumps at T_i, occur at time T_i. It can be seen that this expression is flexible and can be made as simple or as complex as desired for any individual case. It includes as special cases, stepwise, linear and parabolic approximations to $f(t)$.

The Laplace transformation of Equation A-11 is straightforward. It yields

$$F(s) = \sum_{i=1}^{n} \left[\frac{A_i}{s} + \frac{B_i}{s^2} + \frac{2C_i}{s^3} + \frac{6D_i}{s^4} + \ldots \right] e^{-T_i s} \tag{A-12}$$

If the function f(t) is Fourier transformable, $j\omega$ can be substituted for s to give the Fourier transform.

$$F(j\omega) = \sum_{i=1}^{n} \left[\frac{A_i}{j\omega} + \frac{B_i}{-\omega^2} + \frac{2C_i}{-j\omega^3} + \frac{6D_i}{\omega^4} + \ldots \right] e^{-j\omega T_i} \tag{A-13}$$

Now, $F(j\omega)$ can be written in terms of its real and imaginary parts as

$$R(\omega) = \sum_{i=1}^{n} \left[-\frac{A_i}{\omega} + \frac{2C_i}{\omega^3} - \ldots \right] \sin \omega T_i + \left[-\frac{B_i}{\omega^2} + \frac{6D_i}{\omega^4} - \ldots \right] \cos \omega T_i \tag{A-14}$$

$$I(\omega) = \sum_{i=1}^{n} \left[- \frac{A_i}{\omega} + \frac{2C_i}{\omega^3} - \ldots \right] \cos \omega T_i$$

$$- \left[- \frac{B_i}{\omega^2} + \frac{6D_i}{\omega^4} - \ldots \right] \sin \omega T_i \qquad \text{(A-15)}$$

Numerical Fourier Inversion

The symmetry of the Fourier transform pair makes possible the use of Equations A-14 and A-15 for inverse numerical Fourier transformation as well as for evaluation of the direct Fourier transform. Since f(t) is real and zero for negative t, Equation A-5 can be rewritten as shown below:

$$f(t) = \frac{1}{\pi} \int_0^\infty F(j\omega)\, e^{j\omega t}\, d\omega \qquad f(t) = \text{Real} \qquad \text{(A-5)}$$

$$f(t) = \frac{2}{\pi} \int_0^\infty R(\omega) \cos \omega t \, d\omega \qquad \text{(A-16)}$$

$$f(t) = -\frac{2}{\pi} \int_0^\infty I(\omega) \sin \omega t \, d\omega \qquad \text{(A-17)}$$

The similarity of the above integrals and those given in Equation A-9 suggest that Equations A-14 and A-15 be treated simply as quadrature formulae. Thus, R(ω) can be written

$$R(\omega) = \sum_{i=1}^{n} u(\omega - W_i) \left[A_i + B_i(\omega - W_i) + C_i(\omega - W_i)^2 + D_i(\omega - W_i)^3 + \ldots\right] \tag{A-18}$$

where A_i, B_i, etc., now define the discontinuities in $R(\omega)$ and its derivatives. Therefore,

$$f(t) = \frac{2}{\pi} \sum_{i=1}^{n} \left[-\frac{A_i}{t} + \frac{2C_i}{t^3} - \ldots\right] \sin tW_i - \left[-\frac{B_i}{t^2} + \frac{6D_i}{t^4} - \ldots\right] \cos tW_i \tag{A-19}$$

In like manner $I(\omega)$ can be written

$$I(\omega) = \sum_{i=1}^{n} u(\omega - W_i) \left[A_i + B_i(\omega - W_i) + C_i(\omega - W_i)^2 + D_i(\omega - W_i)^3 + \ldots\right] \tag{A-20}$$

where A_i, B_i, etc., here define the discontinuities in $I(\omega)$ and its derivatives.

Thus, f(t) is given by

$$f(t) = \sum_{i=1}^{n} \left[-\frac{A_i}{t} + \frac{2C_i}{t^3} - \cdots \right] \cos tW_i - \left[-\frac{B_i}{t^2} + \frac{6D_i}{t^4} - \cdots \right] \sin t W_i \qquad \text{(A-21)}$$

The relative advantages of using either Equation A-19 or A-21 for the evaluation of f(t) have been discussed by Clements (8). In general, it is better to use Equation A-21 for functions that have no discontinuity at the origin, while Equation A-19 is better suited for inversion of functions with such a discontinuity.

Example of Frequency Domain Model Evaluation

As a simple example of evaluation of a model in the frequency domain, consider the differential equation

$$T \frac{dy}{dt} + y = x(t) \qquad \text{(A-22)}$$

This equation describes the response of a linear first order system excited by some arbitrary input x(t). The Laplace transform solution is

$$Y(s) = X(s) \left(\frac{1}{Ts + 1} \right) \qquad \text{(A-23)}$$

Substitution of $j\omega$ for s gives the Fourier transform solution

$$Y(j\omega) = X(j\omega) \left(\frac{1}{j\omega T + 1} \right) \qquad \text{(A-24)}$$

Substitution of Equation A-24 into Equation A-1 produces the frequency domain expression for ϕ for this particular problem.

$$\phi = \frac{1}{\pi} \int_0^\infty \left| Y_o(j\omega) - X(j\omega) \left(\frac{1}{j\omega T + 1} \right) \right|^2 d\omega \qquad \text{(A-25)}$$

An approximation by linear segments, which is usually satisfactory for the above integral, yields

$$\phi = \frac{\Delta\omega}{\pi} \sum_{k=1}^{m} \left| Y_o(j\omega_k) - X(j\omega_k) \left(\frac{1}{j\omega_k T + 1} \right) \right|^2 \qquad \text{(A-26)}$$

Figure 15 shows the experimental response observed when an analog simulation of a perfectly mixed tank was excited by a triangular input pulse of one second duration and unit height. It is desired to make a least squares comparison of the observed response and the response predicted by a first order system. For the purpose of illustration, this response can be approximated by only three linear segments. Table 11 shows how the coefficients in

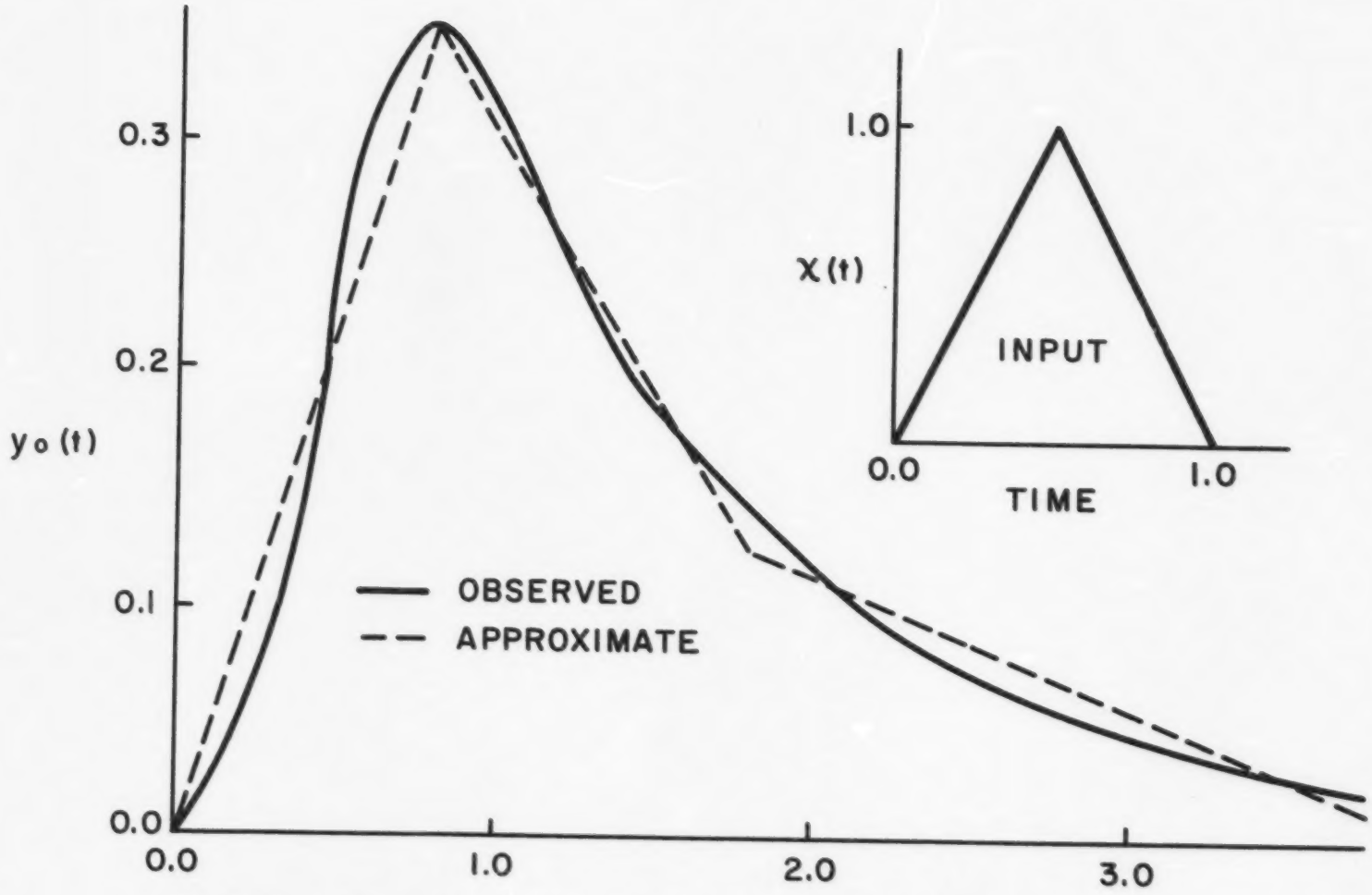

FIGURE 15 RESPONSE OF 1/(TS+1) TO A TRIANGULAR PULSE

TABLE 11

CALCULATION OF RESPONSE DISCONTINUITIES

BREAK POINT	OBSERVED RESPONSE	SEGMENT	SLOPE	SLOPE CHANGE	INDEX
T_i	$y_o(t)$			B_i	i
0	0			0.425	1
		1	0.425		
0.8 sec	0.34			-0.645	2
		2	-0.22		
1.8 sec	0.12			0.165	3
		3	-0.0546		
4.0 sec	0			0.0546	4

Equations A-14 and A-15 are calculated from the linear approximations. This table can be used to write the Fourier transform of the observed response as

$$Y_o(j\omega) = -\frac{1}{\omega^2}(0.425 - 0.645\cos 0.8\omega + 0.165\cos 1.8\omega + 0.0546\cos 4.0\omega) + \frac{j}{\omega^2}(-0.645\sin 0.8\omega + 0.165\sin 1.8\omega + 0.0546\sin 4.0\omega) \quad \text{(A-27)}$$

Likewise, the Fourier transform of the input triangular pulse can be written by inspection as

$$X(j\omega) = -\frac{1}{\omega^2}(2 - 4\cos .5\omega + 2\cos\omega) + \frac{j}{\omega^2}(-4\sin .5\omega + 2\sin\omega) \quad \text{(A-28)}$$

These equations do not give the values of $Y_o(j\omega)$ and $X(j\omega)$ for $\omega = 0$. These values must be calculated from the area under the respective $y_o(t)$ and $x(t)$ curves.

The values of ω to be used in Equation A-26 are selected to range from $\omega = 0$ to some maximum value determined by the criterion

$$\frac{|Y_o(j\omega)|_{\omega=\omega max}}{|Y_o(j\omega)|_{\omega=0}} \approx 0.02 \quad \text{(A-29)}$$

The above equation and Equation A-27 give $\omega_{max} = 0.68$ rad/sec. Twenty-five equally spaced ω_k points are chosen using

$\Delta\omega$ = 0.0272 rad./sec. The values of $Y_o(j\omega_k)$ and $X(j\omega_k)$ are calculated at the ω_k, and tabulated. Marquardt's nonlinear least squares program can be used to minimize ϕ as given by Equation A-26 and to find the best value of the system time constant, T. It is important to notice that in the iterative minimization of ϕ, only $1/(j\omega_k T + 1)$ must be recalculated for each adjustment of T. The transforms of the input pulse and the observed response are not dependent on the parameter, T, and are only evaluated once.

Advantages of Frequency Domain Modeling

The most important difficulty in the direct application of the nonlinear least squares technique to time domain expressions for the observed and predicted responses lies in the calculation of the predicted response, $y_p(t)$. For rather simple systems with simple inputs, the calculation of $y_p(t)$ may offer no difficulty. For example, the response of the first order system described by Equation A-22 to a unit step input is easily found to be

$$y_p(t) = 1 - e^{-t/T} \qquad \text{(A-30)}$$

However, for an arbitrary measured input, x(t), the response can only be written as a convolution of the arbitrary signal

with the unit impulse response.

$$y_p(t) = x(t) * \frac{e^{-t/T}}{T} \qquad \text{(A-31)}$$

or

$$y_p(t) = \int_o^t \frac{e^{-(t-T)/T}}{T}\, dT \qquad \text{(A-32)}$$

If this method for the calculation of $y_p(t)$ is used in conjunction with the time domain minimization of ϕ, it is necessary to perform numerically the integration in Equation A-32 for each time point for each iterated value of the parameter T. For a more complicated model with a large number of parameters this can be a quite time consuming process, particularly when compared to the calculation of $Y_p(j\omega)$ in the frequency domain. The convolution indicated by Equations A-31 and A-32 becomes multiplication when these expressions are transformed to the frequency domain.

$$Y_p(j\omega) = X(j\omega)\left(\frac{1}{j\omega T + 1}\right) \qquad \text{(A-33)}$$

Thus, for arbitrary inputs, the ease with which $Y_p(j\omega)$ can be evaluated makes the frequency domain minimization of ϕ much faster and simpler.

Another important advantage in frequency domain modeling is the facility with which analytical frequency solutions can be obtained as compared with time solutions. The solutions in Chapter 5 illustrate this quite clearly. The frequency solutions of the partial differential equations offer no special problems. However, the analytical inversion of the frequency solutions to find the time solutions is formidable. Also, it is quite likely that such time solutions would contain definite integrals of untabulated functions that would present special numerical evaluation problems.

The region of interest over which it is desired to fit a mathematical model is quite often conveniently expressed in the frequency domain. Frequency domain model evaluation allows one to take this into consideration by modifying the limits of the integral of the squared error to include only the region of interest. This may involve the elimination of a high or low frequency range or the rejection of a band of frequencies that perhaps contains noise or a spurious frequency component. In certain cases it may be desirable to weight the deviations as a function of frequency.

Conclusions

Mathematical modeling is usually thought of as being concerned with time domain signals. However, for many problems it is much simpler and computationally advantageous to evaluate the model in the frequency domain. Indeed, for some problems it may be the only feasible approach. Another distinct advantage of frequency domain regression is that frequency domain specifications and restrictions can be easily incorporated.

The numerical Fourier transformation equations involved in frequency domain modeling are ideally suited for machine computation. This makes it possible to construct generalized computer programs useful in a broad class of problems, thus reducing the time and effort expended on specialized programs for individual modeling problems.

Nomenclature for Appendix A

A, B, C, D	-	Coefficients defined by Equations A-11, A-18 and A-20
F	-	Arbitrary function of frequency
f	-	Arbitrary function of time
I	-	Imaginary part of a complex function
i	-	Summation index

j	-	$\sqrt{-1}$
k	-	Summation index
m	-	Number of ω modeling points
n	-	Number of discontinuities
o	-	Subscript for observed function
p	-	Subscript for predicted function
R	-	Real part of a complex function
s	-	Laplace transform variable
T	-	Time of a discontinuity
T	-	System time constant
t	-	Time
T	-	Integration variable
u	-	Unit step representation
ϕ	-	Integral squared error
W	-	Frequency of a discontinuity
ω	-	Radian frequency
X	-	Fourier transform of input pulse
x	-	Input pulse
Y	-	Fourier transform of output pulse
y	-	Output pulse

APPENDIX B

MODEL-PROTOTYPE SCALE RELATIONS[1]

The inherent restrictions between parameters in scaled models can be derived from the equations of fluid mechanics. Two equations govern the behavior of the viscous flow of pure isothermal fluids: the equation of motion, based upon conservation of momentum, and the equation of continuity, based on the conservation of mass.

For constant μ and ρ, the equation of motion becomes the Navier-Stokes equation,

$$\rho \frac{D\bar{v}}{Dt} = -\nabla p + \mu\nabla^2\bar{v} + \rho g \qquad \text{(B-1)}$$

For the x component this equation can be written

$$\rho\left(\frac{\partial v_x}{\partial t} + v_x \frac{\partial v_x}{\partial x} + v_y \frac{\partial v_x}{\partial y} + v_z \frac{\partial v_x}{\partial z}\right) =$$

$$-\frac{\partial p}{\partial x} + \mu\left(\frac{\partial^2 v_x}{\partial x^2} + \frac{\partial^2 v_x}{\partial y^2} + \frac{\partial^2 v_x}{\partial z^2}\right) + \rho g_x \qquad \text{(B-2)}$$

---

[1] Nomenclature for Appendix B is unique and is listed at the end of Appendix B.

The equation of continuity becomes for constant μ and ρ

$$\frac{\partial v_x}{\partial x} + \frac{\partial v_y}{\partial y} + \frac{\partial v_z}{\partial z} = 0 \qquad \text{(B-3)}$$

If a characteristic length and velocity are selected for a given system, it is possible to write the above equations in terms of dimensionless variables.

$$v_x^* = \frac{v_x}{V} \qquad p^* = \frac{p}{\rho V^2} \qquad t^* = \frac{tV}{L}$$

$$x^* = \frac{x}{L_x} \qquad y^* = \frac{y}{L_y} \qquad z^* = \frac{z}{L_z} \qquad \text{(B-4)}$$

An attempt has been made to select a number of different characteristic lengths; however, it can be demonstrated that all lengths must be identical, as follows:

$$v_x = \frac{dx}{dt} = \frac{d(L_x\, x^*)}{d(\frac{L}{V}\, t^*)} = \frac{L_x}{L}\, V \frac{dx^*}{dt^*} \qquad \text{(B-5)}$$

or

$$v_x = \frac{L_x}{L} Vv^* \qquad \text{(B-6)}$$

but v_x must equal Vv^* and therefore: L_x must equal L. In a similar manner, $L_x = L_y = L_z = L$ and only one characteristic length is allowed.

Substitution into the x component of the Navier-Stokes equation yields:

$$\rho\left(\frac{V^2}{L}\frac{\partial v_x^*}{\partial t^*} + \frac{V^2}{L}v_x^*\frac{\partial v_x^*}{\partial x^*} + \frac{V^2}{L}v_y^*\frac{\partial v_x^*}{\partial y^*} + \frac{V^2}{L}v_z^*\frac{\partial v_x^*}{\partial z^*}\right) =$$

$$-\frac{\rho V^2}{L}\frac{\partial p^*}{\partial x^*} + \mu\left(\frac{V}{L^2}\frac{\partial^2 v_x^*}{\partial x^{*2}} + \frac{V}{L^2}\frac{\partial^2 v_x^*}{\partial y^{*2}} + \frac{V}{L^2}\frac{\partial^2 v_x^*}{\partial z^{*2}}\right) + \rho g_x \qquad \text{(B-7)}$$

or

$$\frac{\partial v_x^*}{\partial t^*} + v_x^*\frac{\partial v_x^*}{\partial x^*} + v_y^*\frac{\partial v_x^*}{\partial y^*} + v_z^*\frac{\partial v_x^*}{\partial z^*} =$$

$$\frac{\partial p^*}{\partial x^*} + \left[\frac{\mu}{\rho LV}\right]\left(\frac{\partial^2 v_x^*}{\partial x^{*2}} + \frac{\partial^2 v_x^*}{\partial y^{*2}} + \frac{\partial^2 v_x^*}{\partial z^{*2}}\right) + \left[\frac{Lg_x}{V^2}\right] \qquad \text{(B-8)}$$

The first term in brackets is observed to be the Reynolds Number and the second term in brackets, the Froude Number. It may therefore be concluded that for dynamic similarity of two systems, the following three relationships must hold:

$$\frac{L_{x1}}{L_{x2}} = \frac{L_{y1}}{L_{y2}} = \frac{L_{z1}}{L_{z2}} = \frac{L_1}{L_2} \qquad \text{Geometric Similarity}$$

$$\frac{L_1 V_1 \rho_1}{\mu_1} = \frac{L_2 V_2 \rho_2}{\mu_2} \qquad \text{Reynolds Number}$$

$$\frac{L_1 g_1}{V_1^2} = \frac{L_2 g_2}{V_2^2} \qquad \text{Froude Number}$$

(B-9)

Since gravity cannot usually be varied and the velocity is a dependent variable, these relationships can be reduced to the following.

$$\nu_2 = \nu_1 \, (L_2/L_1)^{3/2} \qquad \text{(B-10)}$$

Application of this result to the scaling of flow in rivers and streams indicates that a very low viscosity liquid must be used in the scaled-down model. For scaled-down factors of twenty or thirty to one the kinematic viscosity of the liquid used in the model would have to be about one hundred times less than the kinematic viscosity of water. Unfortunately there is no liquid with such a low kinematic viscosity that would be practical for modeling applications.

Nomenclature for Appendix B

D	Indicates substantial derivative
∇	Del or nabula operator
g	Acceleration of gravity
L	Characteristic length
μ	Viscosity
ν	Kinematic viscosity
p	Pressure
ρ	Density
t	Time
V	Characteristic velocity
v	Velocity
x, y, z	Spatial coordinates
1, 2	Subscripts for prototype and model

APPENDIX C

DISPERSED FLOW AND DEAD ZONE MODEL PARAMETERS: CHANNEL EXPERIMENTS

IDENT.	BRICKS	T	T	β	T_d	SE	F
H 2B	NONE	0.01307	36.4			0.027	
H 2B	NONE	0.00995	36.8	0.041	0.060	0.018	2.15
H 3C	NONE	0.01307	36.2			0.022	
H 3C	NONE	0.01015	36.5	0.039	0.051	0.014	2.65
H 4A	NONE	0.01439	41.1			0.027	
H 4A	NONE	0.01149	41.4	0.035	0.060	0.024	1.34
H 5B	NONE	0.01333	40.4			0.028	
H 5B	NONE	0.00881	41.0	0.059	0.053	0.015	3.33
H 6C	NONE	0.01399	40.6			0.022	
H 6C	NONE	0.01183	41.0	0.025	0.072	0.014	2.45
H 7A	NONE	0.01361	43.5			0.028	
H 7A	NONE	0.00995	44.0	0.051	0.048	0.020	1.99
H 8B	NONE	0.01389	43.7			0.027	
H 8A	NONE	0.01031	44.2	0.046	0.053	0.020	1.93
H 9C	NONE	0.01389	43.9			0.021	
H 9C	NONE	0.00885	44.5	0.070	0.047	0.009	6.13
H 10A	NONE	0.01361	38.6			0.029	
H 10	NONE	0.01087	39.0	0.035	0.055	0.021	1.88
H 11B	NONE	0.01379	38.4			0.024	
H 11	NONE	0.01047	38.8	0.043	0.055	0.016	2.39
H 15BD	2S	0.01639	36.7			0.033	
H 15BD	2S	0.00820	37.5	0.097	0.054	0.011	9.06

IDENT.	BRICKS	T	T	β	T_d	SE	F
H 16C	2S	0.01653	36.0			0.040	
H 16C	2S	0.00746	36.8	0.110	0.053	0.019	4.50
H 17A	3S	0.01835	35.0			0.048	
H 17A	3S	0.00717	36.0	0.124	0.058	0.016	9.35
H 19C	3S	0.01515	34.9			0.043	
H 19C	3S	0.00656	35.8	0.101	0.059	0.005	66.75
H 26A	4S	0.01887	32.3			0.048	
H 26A	4S	0.01143	33.5	0.071	0.107	0.016	8.64
H 27B	4S	0.01835	33.3				
H 27B	4S	0.00957	34.1	0.094	0.065	0.019	4.44
H 28C	4S	0.01709	32.8			0.054	
H 28C	4S	0.00980	33.7	0.077	0.076	0.040	1.89
H 35A	5S	0.01770	36.3			0.037	
H 35A	5S	0.00702	37.4	0.122	0.055	0.008	22.59
H 36B	5S	0.01869	36.2			0.042	
H 36B	5S	0.00784	37.5	0.113	0.067	0.017	6.15
H 37C	5S	0.01905	36.1			0.042	
H 37C	5S	0.00794	37.2	0.122	0.060	0.020	4.43
H 43A	6S	0.02022	36.0			0.042	
H 43A	6S	0.00787	37.2	0.127	0.065	0.014	9.04
H 44B	6S	0.01980	35.2			0.052	
H 44B	6S	0.00667	36.6	0.130	0.070	0.012	19.39
H 45C	6S	0.01923	35.4			0.053	
H 45C	6S	0.00645	36.9	0.128	0.073	0.013	16.37
H 49A	7S	0.02073	34.0			0.054	
H 49A	7S	0.00719	35.6	0.127	0.079	0.013	16.98
H 50B	7S	0.02081	33.8			0.069	
H 50B	7S	0.00654	35.6	0.129	0.091	0.014	25.15

IDENT	BRICKS	T	T	β	T_d	SE	F
H 51C	7S	0.02004	33.8			0.061	
H 51C	7S	0.00649	35.4	0.127	0.080	0.010	38.11
H 57A	8S	0.02077	33.7			0.053	
H 57A	8S	0.00873	35.1	0.111	0.086	0.009	32.03
H 58B	8S	0.02275	33.7			0.061	
H 58B	8S	0.00833	35.5	0.127	0.095	0.011	32.71
H 64B	9S	0.02710	35.7			0.050	
H 64B	9S	0.00781	37.5	0.163	0.080	0.013	16.26
H 65C	9S	0.02833	35.9			0.060	
H 65C	10S	0.00787	38.0	0.167	0.090	0.020	9.09
H 71A	10S	0.02621	33.7			0.068	
H 71A	10S	0.00971	36.0	0.133	0.120	0.017	15.72
H 72B	10S	0.02674	33.5			0.058	
H 72B	10S	0.00930	35.4	0.142	0.096	0.016	13.32
H 79A	12S	0.02535	32.8			0.072	
H 79A	12S	0.00897	35.0	0.136	0.118	0.015	22.67
H 80B	12S	0.03021	33.3			0.060	
H 80B	12S	0.00976	35.4	0.155	0.104	0.022	7.79
H 87A	14S	0.03317	33.4			0.065	
H 87A	14S	0.01015	35.8	0.162	0.118	0.009	54.06
H 88B	14S	0.03527	33.8			0.063	
H 88B	14S	0.01015	36.4	0.172	0.118	0.016	16.26
H 95A	16S	0.03610	34.5			0.068	
H 95A	16S	0.00905	37.5	0.183	0.123	0.016	19.11
H 96B	16S	0.02882	33.8			0.080	
H 96B	16S	0.00758	36.5	0.160	0.120	0.010	68.36
H101A	18S	0.04057	32.0			0.082	
H101A	18S	0.01325	35.9	0.182	0.196	0.013	38.59

IDENT.	BRICKS	T	T	β	T_d	SE	F
H102B	18S	0.03766	31.8			0.094	
H102B	18S	0.01212	36.1	0.185	0.208	0.024	15.37
H109A	20S	0.04545	33.1			0.095	
H109A	20S	0.00976	37.6	0.209	0.181	0.010	92.82
H110B	20S	0.03617	31.8			0.088	
H1108	20S	0.00885	35.1	0.183	0.147	0.012	57.68
HSKPA	20S	0.03731	31.2			0.090	
HSKPA	20S	0.00948	34.7	0.180	0.161	0.009	92.28
HSKPB	20S	0.03591	31.5			0.087	
HSKPB	20S	0.00893	34.7	0.184	0.141	0.015	33.95
H115A	22S	0.04662	33.7			0.091	
H115A	22S	0.00905	38.1	0.217	0.172	0.016	32.06
H116B	22S	0.04032	33.2			0.097	
H116B	22S	0.00820	37.2	0.201	0.160	0.013	55.22
H117A	22S	0.04024	32.9			0.099	
H117A	22S	0.00870	37.1	0.204	0.165	0.013	56.88
H118B	22S	0.03817	33.0			0.093	
H118B	22S	0.00905	36.8	0.190	0.164	0.015	39.29
H125A	24S	0.04673	31.7			0.109	
H125A	24S	0.00939	36.7	0.222	0.203	0.011	101.86
H127A	24S	0.04283	32.1			0.088	
H127A	24S	0.01010	36.1	0.202	0.170	0.009	92.12
H128B	24S	0.05000	31.9			0.099	
H128B	24S	0.00995	36.3	0.224	0.180	0.015	45.79
H133A	26S	0.04556	30.9			0.105	
H133A	26S	0.01042	35.5	0.208	0.210	0.013	64.73
H134B	26S	0.04008	30.1			0.101	
H134B	26S	0.01010	34.2	0.197	0.189	0.015	46.66

IDENT.	BRICKS	T	T	β	T_d	SE	F
H146A	28S	0.04926	32.8			0.087	
H146A	28S	0.01058	37.2	0.219	0.177	0.009	83.66
H148B	28S	0.03960	29.5			0.115	
H148B	28S	0.00935	34.2	0.209	0.213	0.013	80.86
H149A	30S	0.04843	28.4			0.103	
H149A	30S	0.01156	33.0	0.220	0.214	0.010	111.11
H150B	30S	0.04728	28.6			0.114	
H150B	30S	0.00926	33.3	0.227	0.206	0.011	112.20
H163A	38S	0.05900	35.8			0.102	
H163A	38S	0.01205	41.6	0.240	0.210	0.014	52.56
H164B	38S	0.05089	35.3			0.105	
H164B	38S	0.01136	41.0	0.224	0.215	0.017	40.42
H165A	42S	0.06494	34.9			0.123	
H165A	42S	0.01075	43.7	0.289	0.275	0.015	65.91
H166B	42S	0.05435	35.2			0.117	
H166B	42S	0.00957	41.7	0.248	0.219	0.014	73.38
H 32A	4SBS	0.02000	37.0			0.045	
H 32A	4SBS	0.00858	38.3	0.112	0.075	0.011	16.29
H 33B	4SBS	0.02110	36.9			0.045	
H 33B	4SBS	0.00855	38.3	0.120	0.075	0.015	9.37
H 34C	4SBS	0.02130	37.1			0.045	
H 34C	4SBS	0.00866	38.4	0.124	0.071	0.015	8.96
H 46A	6SBS	0.01942	35.7			0.044	
H 46A	6SBS	0.00658	37.0	0.137	0.060	0.012	13.20
H 47B	6SBS	0.01905	34.7			0.048	
H 47B	6SBS	0.00604	35.9	0.139	0.060	0.013	13.26
H 48C	6SBS	0.02358	35.3			0.049	
H 48C	6SBS	0.00704	36.8	0.153	0.070	0.014	12.53

IDENT.	BRICKS	T	T	θ	T_d	SE	F
H 60A	8SBS	0.02132	32.4			0.056	
H 60A	8SBS	0.00707	33.9	0.131	0.079	0.004	197.40
H 61B	8SBS	0 02541	33.2			0.041	
H 61B	8SBS	0.00813	34.6	0.165	0.066	0.015	7.92
H 62C	8SBS	0.02554	33.7			0.047	
H 62C	8SBS	0.00746	35.2	0.162	0.072	0.014	16.14
H 73AD	10SBS	0.02528	33.8			0.068	
H 73AD	10SBS	0.00826	36.0	0.139	0.108	0.009	57.09
H 81A	12SBS	0.02911	33.9			0.069	
H 81A	12SBS	0.00639	36.2	0.176	0.096	0.010	49.14
H 83A	12SBS	0.02721	34.6				
H 83A	12SBS	0.00930	37.1	0.140	0.116	0.010	49.58
H 84B	12SBS	0.02946	34.7			0.073	
H 84B	12SBS	0.00816	37.1	0.158	0.112	0.017	19.32
H 85A	14SBS	0.02990	33.4			0.080	
H 85A	14SBS	0.00922	36.3	0.155	0.138	0.011	50.37
H 86B	14SBS	0.03515	34.1			0.087	
H 86B	14SBS	0.00962	37.8	0.177	0.156	0.020	19.13
H 97A	16SBS	0.03604	33.4			0.075	
H 97A	16SBS	0.01070	36.3	0.170	0.143	0.009	66.64
H 98B	16SBS	0.03724	32.8			0.083	
H 98B	16SBS	0.00966	36.1	0.180	0.146	0.024	11.99
H 99A	18SBS	0.03610	33.7			0.088	
H 99A	18SBS	0.00962	37.2	0.180	0.156	0.015	36.67
H100B	18SBS	0.03565	33.8			0.090	
H100B	18SBS	0.00851	37.4	0.180	0.155	0.009	94.64
H111A	22SBS	0.04149	31.8			0.098	
H111A	22SBS	0.00976	36.1	0.201	0.183	0.014	47.14

IDENT.	BRICKS	T	T	β	T_d	SE	F
H112B	22SBS	0.03643	31.7			0.092	
H112B	22SBS	0.01047	35.6	0.183	0.177	0.017	30.09
H114B	22SBS	0.03597	32.4			0.102	
H114B	22SBS	0.00816	36.4	0.188	0.166	0.015	45.18
H129A	24SBS	0.03490	31.3			0.102	
H129A	24SBS	0.00905	34.8	0.178	0.168	0.016	38.53
H130B	24SBS	0.03333	32.0			0.090	
H130B	24SBS	0.00858	35.3	0.185	0.145	0.012	58.78
H131A	26SBS	0.03252	31.3			0.102	
H131A	26SBS	0.00840	34.9	0.178	0.169	0.013	66.85
H132B	26SBS	0.03656	31.4			0.096	
H132B	26SBS	0.01026	35.2	0.180	0.181	0.012	66.76
H151A	30SBS	0.03279	28.2			0.109	
H151A	30SBS	0.00889	31.8	0.179	0.181	0.011	105.35
H153A	30SBS	0.04843	29.7			0.115	
H153A	30SBS	0.01047	35.1	0.231	0.231	0.014	73.07
H154B	30SBS	0.03810	28.8			0.110	
H154B	30SBS	0.01070	33.2	0.198	0.217	0.019	32.99
H155A	32SBS	0.05714	28.3			0.121	
H155A	32SBS	0.01099	33.9	0.250	0.238	0.016	55.01
H156B	32SBS	0.04728	28.5			0.101	
H156B	32SBS	0.01010	32.4	0.214	0.186	0.010	112.58
H157A	32SBS	0.04598	35.0			0.098	
H157A	32SBS	0.00926	40.1	0.218	0.187	0.015	40.83
H158B	32SBS	0.04310	35.2			0.098	
H158B	32SBS	0.01064	40.6	0.208	0.213	0.011	82.34
H159A	34SBS	0.03656	35.2			0.104	
H159A	34SBS	0.00858	40.5	0.202	0.200	0.013	61.38

IDENT.	BRICKS	T_1	T_2	β	T_d	SE	F
H160	34SBS	0.04854	35.1			0.099	
H160	34SBS	0.01036	41.0	0.228	0.212	0.012	67.21
H161A	38SBS	0.04193	34.2			0.109	
H161A	38SB*	0.01550	40.0	0.198	0.267	0.043	6.40
H162B	38SBS	0.04598	34.1			0.118	
H162B	38SBS	0.01093	40.1	0.223	0.232	0.011	112.05
H167A	42SBS	0.05540	35.5			0.105	
H167A	42SBS	0.01070	42.0	0.248	0.223	0.018	33.85
H168B	42SBS	0.06211	36.4			0.118	
H168B	42SBS	0.01036	43.7	0.264	0.235	0.008	216.09
H 13A	1SS	0.01449	35.7			0.037	
H 13A	1SS	0.00971	36.4	0.055	0.078	0.019	3.77
H 14B	1SS	0.01538	35.6			0.040	
H 14B	1SS	0.00905	36.3	0.072	0.064	0.020	3.90
H 15C	1SS	0.01399	35.5			0.037	
H 15C	1SS	0.00855	36.4	0.066	0.069	0.013	8.18
H 20A	3SS	0.01527	34.4			0.046	
H 20A	3SS	0.00673	35.3	0.102	0.059	0.019	6.21
H 21B	3SS	0.01786	34.8			0.059	
H 21B	3SS	0.00784	36.3	0.096	0.093	0.015	15.01
H 22C	3SS	0.01961	33.5			0.061	
H 22C	3SS	0.00797	36.2	0.108	0.097	0.010	38.87
H 23A	2SS	0.01550	34.3			0.056	
H 23A	2SS	0.00806	35.6	0.084	0.092	0.020	7.54
H 24B	2SS	0.01905	33.9			0.060	
H 24B	2SS	0.00813	35.3	0.104	0.090	0.014	18.93
H 25C	2SS	0.01538	34.2			0.052	
H 25C	2SS	0.00678	35.3	0.095	0.070	0.011	22.43

IDENT.	BRICKS	T	T	β	T_d	SE	F
H 29C	4SS	0.02012	36.2			0.064	
H 29C	4SS	0.01015	37.3	0.090	0.085	0.029	4.80
H 30B	4SS	0.01905	36.0			0.048	
H 30B	4SS	0.00930	37.2	0.097	0.075	0.018	6.74
H 31C	4SS	0.01653	35.9			0.061	
H 31C	4SS	0.00826	37.4	0.085	0.091	0.015	15.79
H 38A	5SS	0.01587	34.6			0.051	
H 38A	5SS	0.00755	35.9	0.093	0.076	0.022	5.61
H 39B	5SS	0.01724	34.6			0.062	
H 39B	5SS	0.00766	36.1	0.097	0.091	0.022	8.34
H 40CD	5SS	0.01681	34.9			0.057	
H 40CD	5SS	0.00763	36.3	0.093	0.089	0.011	26.18
H 40AD	6SS	0.01527	34.5			0.047	
H 40AD	6SS	0.00697	35.2	0.120	0.038	0.037	1.56
H 41B	6SS	0.01786	34.8			0.057	
H 41B	6SS	0.00692	36.2	0.122	0.077	0.016	13.20
H 42C	6SS	0.01770	34.9			0.052	
H 42C	6SS	0.00749	36.3	0.105	0.078	0.020	7.04
H 52A	7SS	0.01408	32.2			0.067	
H 52A	7SS	0.00971	33.6	0.095	0.082	0.032	4.58
H 53B	7SS	0.02000	33.7			0.081	
H 53B	7SS	0.00855	35.7	0.104	0.129	0.031	7.00
H 54C	7SS	0.02299	33.3			0.085	
H 54C	7SS	0.00733	35.7	0.133	0.124	0.013	43.58
H 54AD	8SS	0.01923	33.4			0.081	
H 54AD	8SS	0.00820	35.8	0.118	0.137	0.020	16.12
H 55B	8SS	0.01626	32.7			0.076	
H 55B	8SS	0.00699	34.3	0.097	0.101	0.020	15.31

IDENT.	BRICKS	T	T	β	T_d	SE	F
H 56C	8SS	0.01538	32.3			0.061	
H 56C	8SS	0.00717	33.8	0.090	0.096	0.022	7.61
H 66A	9SS	0.02494	34.1			0.095	
H 66A	9SS	0.00791	37.5	0.154	0.151	0.023	17.60
H 67B	9SS	0.02364	33.9			0.084	
H 67B	9SS	0.00826	36.8	0.136	0.147	0.015	33.24
H 68C	9SS	0.02123	33.3			0.084	
H 68C	9SS	0.00784	35.9	0.124	0.136	0.009	80.81
H 69A	10SS	0.02564	33.4			0.096	
H 69A	10SS	0.00943	36.7	0.144	0.170	0.022	19.20
H 70B	10SS	0.01575	33.1			0.079	
H 70B	10SS	0.00769	35.3	0.098	0.138	0.014	28.95
H 75AD	12SS	0.01709	31.5			0.080	
H 75AD	12SS	0.00800	33.7	0.100	0.147	0.025	10.05
H 77A	12SS	0.01786	30.7			0.080	
H 77A	12SS	0.00823	32.7	0.102	0.142	0.017	22.45
H 78B	12SS	0.01869	30.6			0.081	
H 78B	12SS	0.00935	33.0	0.105	0.166	0.019	17.84
H 89A	14SS	0.02227	31.6			0.100	
H 89A	14SS	0.01026	36.0	0.152	0.259	0.023	19.29
H 91A	14SS	0.02538	31.3			0.094	
H 91A	14SS	0.01143	36.9	0.179	0.316	0.018	27.22
H 92B	14SS	0.01905	32.3			0.091	
H 92B	14SS	0.00990	36.1	0.128	0.272	0.014	44.12
H 93A	16SS	0.02030	31.8			0.099	
H 93A	16SS	0.01053	36.0	0.137	0.300	0.020	24.07
H 94B	16SS	0.02083	31.4			0.096	
H 94B	16SS	0.00893	35.0	0.139	0.216	0.017	30.86

IDENT.	BRICKS	T	T	β	T_d	SE	F
H103A	18SS	0 01587	31.1			0.086	
H103A	18SS	0.00930	33.3	0.087	0.201	0.026	11.16
H105A	18SS	0.01754	31.5			0.078	
H105A	18SS	0.00995	33.6	0.090	0.193	0.027	8.25
H106B	18SS	0.02121	31.4			0.099	
H106B	18SS	0.00926	34.7	0.133	0.203	0.021	22.65
H107A	20SS	0.02500	31.5			0.112	
H107A	20SS	0.01031	35.9	0.160	0.257	0.021	29.85
H108B	20SS	0.02167	31.2			0.118	
H108B	20SS	0.00939	36.5	0.172	0.308	0.020	34.64
H119A	22SSV	0.02018	37.3			0.081	
H119A	22SSV	0.00995	40.7	0.116	0.207	0.020	16.69
H120B	22SSC	0.02018	37.3			0.075	
H120B	22SSC	0.00995	40.7	0.116	0.207	0.021	13.11
H121A	22SS	0.02028	31.1			0.098	
H121A	22SS	0.00995	34.3	0.125	0.229	0.023	17.92
H122B	22SS	0.02475	31.3			0.115	
H122B	22SS	0.01005	35.5	0.158	0.259	0.036	10.15
H123A	24SS	0.01980	30.2			0.106	
H123A	24SS	0.01010	35.0	0.155	0.332	0.022	23.35
H124B	24SS	0.01852	30.1			0.093	
H124B	24SS	0.00966	34.0	0.133	0.290	0.020	20.92
H137B	26SS	0.01379	28.6			0.078	
H137A	26SS	0.00913	31.1	0.092	0.293	0.026	9.09
H138A	26SS	0.01538	30.5			0.078	
H138A	26SS	0.00935	33.6	0.107	0.296	0.023	11.42
H139B	26SS	0.01587	30.0				
H139B	26SS	0.00985	33.4	0.113	0.325	0.025	12.24

IDENT.	BRICKS	T	T	-β	T_d	SE	F
H140A	28SS	0.01550	38.9			0.051	
H140A	28SS	0.01176	40.5	0.052	0.230	0.022	5.25
H141B	28SS	0.01515	40.1			0.053	
H141B	28SS	0.01111	42.1	0.061	0.234	0.016	11.31
H142A	28SS	0.01307	32.4			0.055	
H142A	28SS	0.00930	33.9	0.059	0.195	0.021	7.07
H143B	2BSS	0.01538	30.9			0.058	
H143B	28SS	0.01105	32.3	0.059	0.208	0.020	8.67
H144A	28SS	0.01370	30.4			0.049	
H144A	28SS	0.00962	31.3	0.050	0.117	0.024	4.36
H145B	28SS	0.01852	30.3			0.076	
H145B	28SS	0.01124	32.6	0.089	0.245	0.024	10.28
H169A	MISC.	0.08511	35.8			0.146	
H169A	MISC.	0.01093	47.5	0.337	0.327	0.012	140.32
H170B	MISC.	0.09259	35.7			0.140	
H170B	MISC.	0.01136	46.7	0.333	0.312	0.015	91.43
H171	MISC.	0.06557	35.1			0.146	
H171	MISC.	0.01250	46.6	0.316	0.351	0.015	95.00
H172	MISC.	0.07663	35.0			0.138	
H172	MISC.	0.01493	44.9	0.303	0.318	0.028	24.71
H173	MISC.	0.23923	42.5			0.106	
H173	MISC.	0.01250	59.7	0.487	0.310	0.015	50.61
H174	MISC.	0.31496	46.7			0.099	
H174	MISC.	0.01163	67.8	0.543	0.320	0.014	54.00
H175	MISC.	0.03175	66.7			0.320	
H175	MISC.	0.03407	83.8	0.590	0.196	0.013	623.44
H176	MISC.	0.10000	40.8			0.136	
H176	MISC.	0.01282	54.9	0.354	0.340	0.013	114.34

IDENT.	BRICKS	T	T	β	T_d	SE	F
H177	MISC.	0.14706	38.6			0.135	
H177	MISC.	0.01183	52.4	0.400	0.330	0.016	74.89
H178A	MISC.	0.03883	35.7			0.104	
H178A	MISC.	0.01205	41.5	0.199	0.242	0.021	25.15
H179B	MISC.	0.03861	36.3			0.107	
H179B	MISC.	0.01036	42.1	0.204	0.226	0.017	42.37
H180A	MISC.	0.03922	34.6			0.123	
H180A	MISC.	0.01250	41.0	0.208	0.280	0.029	17.99
H181B	MISC.	0.05780	34.9			0.139	
H181B	MISC.	0.01449	43.5	0.260	0.291	0.029	23.03
H182	MISC.	0.14599	39.7			0.128	
H182	MISC.	0.01563	54.7	0.399	0.350	0.011	137.26
H183	MISC.	0.02392	42.2			0.107	
H183	MISC.	0.01370	58.3	0.481	0.313	0.016	46.61
H184	MISC.	0.66225	69.7			0.054	
H184	MISC.	0.62751	110.0	0.708	0.303	0.014	15.53
H190	MISC.	0.06098	33.3			0.179	
H190	MISC.	0.01183	56.3	0.439	0.592	0.020	79.31
H191D	MISC.	0.05222	40.2			0.157	
H191D	MISC.	0.01047	63.2	0.399	0.506	0.018	75.24
H191E	MISC.	0.04464	32.2			0.158	
H191E	MISC.	0.01136	52.1	0.408	0.584	0.024	43.34

APPENDIX D

DISPERSED FLOW AND DEAD ZONE MODEL PARAMETERS: RIVER EXPERIMENTS

IDENT.		T	T	β	T_d	SE	F
C	1	0.00255	2684			0.018	
C	1	0.00234	2690	0.007	0.031	0.014	1.65
C	2	0.00615	574			0.024	
C	2	0.00500	579	0.023	0.055	0.010	5.55
C	3	0.00490	611			0.034	
C	3	0.00322	617	0.035	0.036	0.012	7.56
C	5	0.00522	718			0.032	
C	5	0.00366	725	0.033	0.040	0.016	3.93
C	6	0.00190	2452			0.050	
C	6	0.00130	2483	0.021	0.045	0.020	6.23
C	7	0.00186	2807			0.027	
C	7	0.00185	2808	0.005	0.004	0.027	1.01
C	8	0.00403	706			0.041	
C	8	0.00282	713	0.028	0.042	0.024	2.99
C	9	0.00366	709			0.032	
C	9	0.00285	715	0.019	0.047	0.010	10.73
C	10	0.00738	678			0.031	
C	10	0.00602	687	0.024	0.089	0.005	35.08
C	11	0.00535	747			0.036	
C	11	0.00397	785	0.026	0.065	0.005	46.39
C	12	0.00444	2407			0.020	
C	12	0.00444	2407	0.005	0.003	0.019	1.05

IDENT.		T	T	β	T_d	SE	F
C	13	0.00180	2731				
C	13	0.00128	2756	0.018	0.040	0.010	22.35
F	1	0.00388	3827			0.030	
F	1	0.00323	3844	0.016	0.041	0.016	3.24
F	2	0.00337	3787			0.029	
F	2	0.00269	3816	0.016	0.048	0.010	8.94
F	4	0.00255	2371			0.029	
F	4	0.00211	2383	0.013	0.037	0.009	10.02
F	5	0.00304	2291			0.026	
F	5	0.00296	2292	0.003	0.024	0.026	1.00
F	6	0.00246	2355			0.022	
F	6	0.00200	2365	0.013	0.030	0.004	32.11
F	8	0.00365	1680			0.062	
F	8	0.00251	1703	0.022	0.067	0.044	1.98
F	9	0.00273	1689			0.030	
F	9	0.00249	1695	0.007	0.057	0.020	2.11
F	10	0.00352	1462			0.042	
F	10	0.00382	1486	0.020	0.115	0.024	3.07
F	11	0.00308	1397			0.032	
F	11	0.00267	1404	0.010	0.050	0.018	3.01
F	13	0.00301	1425			0.011	
F	13	0.00299	1425	0.002	0.024	0.010	1.12
F	14	0.00239	1529			0.027	
F	14	0.00222	1535	0.008	0.041	0.019	2.11
H	1	0.00952	384			0.044	
H	1	0.00545	392	0.058	0.058	0.013	11.31
H	2	0.00990	390			0.051	
H	2	0.00483	399	0.072	0.059	0.004	198.34

IDENT.		T	T	β	T_d	SE	F
H	3	0.01183	385			0.034	
H	3	0.00797	391	0.050	0.064	0.009	13.01
H	4	0.00833	395			0.025	
H	4	0.00604	398	0.037	0.044	0.010	6.15
H	5	0.00590	450			0.049	
H	5	0.00377	458	0.041	0.053	0.010	24.11
H	6	0.01149	342			0.023	
H	6	0.00837	346	0.044	0.051	0.009	6.45
H	7	0.00826	399			0.028	
H	7	0.00621	404	0.033	0.059	0.005	29.20
H	8	0.00583	380			0.015	
H	8	0.00473	382	0.026	0.028	0.009	2.60
H	9	0.00494	366			0.052	
H	9	0.00303	371	0.037	0.049	0.027	3.78
H	10	0.00612	370			0.030	
H	10	0.00455	373	0.029	0.045	0.012	6.59
H	11	0.00645	376			0.009	
H	11	0.00641	376	0.005	0.002	0.009	0.96
H	12	0.00800	350			0.019	
H	12	0.00619	353	0.031	0.041	0.007	7.81
H	13	0.00694	346			0.023	
H	13	0.00533	348	0.029	0.040	0.011	4.97
H	14	0.00717	348			0.018	
H	14	0.00575	350	0.027	0.035	0.009	3.83
H	15	0.00641	350			0.032	
H	15	0.00471	354	0.037	0.042	0.013	5.83
H	16	0.00585	341			0.030	
H	16	0.00408	344	0.035	0.037	0.013	5.24

IDENT.	T_∞	T	β	T_d	SE	F
H 17	0.00578	346			0.017	
H 17	0.00440	348	0.038	0.021	0.014	1.43
H 18	0.00563	334			0.015	
H 18	0.00513	335	0.009	0.060	0.008	4.05

APPENDIX E

NOMENCLATURE

A_a	Cross-sectional area of the main stream
A_d	Cross-sectional area of the dead zone
a	Ratio of contact area to main stream volume
a	Subscript for main stream
α	Main stream fraction of cross section
α_o	Fraction of measurement or injection made in main stream at x = 0
α_1	Fraction of measurement made in main stream at x = L
B	Arbitrary coefficient
β	Dead zone fraction of cross section
β_o	Fraction of measurement or injection made in dead zone at x = 0
β_1	Fraction of measurement made in dead zone at x = L
C	Transformed concentration
$\overline{C}$	Twice transformed concentration
c_a	Concentration in main stream
c_d	Concentration in dead zone

c_{ao}	Concentration in main stream at x = 0
c_{al}	Concentration in main stream at x = L
c_{av}	Average concentration
c_{dav}	Average concentration in dead zone
c_{mo}	Measured concentration at x = 0
c_{ml}	Measured concentration at x = L
γ	Second coefficient in expansion of ψ
c'	Turbulent concentration fluctuation
$\bar{c}$	Time smoothed concentration
D	Dispersion coefficient
D_a	Dispersion coefficient in main stream
D_d	Dispersion coefficient in dead zone
D^m	Molecular diffusivity
D^t	Turbulent diffusivity
D^{mt}	$D^m + D^t$
d	Ratio of contact area to dead zone volume
d	Subscript for dead zone
δ	Delta function
F	Ratio of dispersed flow SE to dead zone SE
G	See Equation 5-27
h	Mean depth of stream or river

I_o	Bessel function
I_1	Bessel function
j	Square root of minus one
K	Mass transfer coefficient
L	Length of test section
L_d	Depth of dead zone
M	Injection mass
N_a	Mass transport in main stream by dispersion
N_d	Mass transport in dead zone
P	Contact length in any cross section
p	Transform variable (distance)
R	Radius of cylindrical or spherical dead zone
R_o	Transformed injection rate
r	Radial distance in cylindrical and spherical dead zone
r_o	Injection rate
s	Transform variable (time)
S	T_s
SE	Standard error of estimate
Se	Slope of the energy grade line
T	Average residence time of test section
T_d	Average residence time of dead zone

T_{dp}	Average residence time of main stream by dispersion alone
T_v	Average residence time of main stream by velocity alone
t	Time
T	Relative dispersion coefficient = T/T_{dp}
T_d	Relative dead zone holdup = T_d/T
τ_o	Shear stress at the wall
U	Average velocity in main stream
U_*	Defined by Equation 8-2
v_x, v_y, v_z	Velocity components
v'_x, v'_y, v'_z	Turbulent velocity components
$\bar{v}_x, \bar{v}_y, \bar{v}_z$	Time-smoothed velocity components
ω	Radian frequency
x, y, z	Space coordinates

LIST OF REFERENCES

1. Aris, R., Proc. Roy. Soc., A235, 67 (1956).

2. Bellman, R., Adaptive Control Processes: A Guided Tour, Princeton University Press, Princeton, New Jersey, 1961.

3. Bird, R. B., Stewart, W. E., and Lightfoot, E. M., Transport Phenomena, John Wiley and Sons, New York, 1960.

4. Bugliarello, G., and Jackson, E. D., III, "A Random Walk Study of Convective Diffusion," ASCE Water Resources Engineering Conference, 1963.

5. Churchill, M. A., Buckingham, R. A., and Elmore, H. L., "The Prediction of Stream Reareation Rates," Tennessee Valley Authority, Chattanooga, Tennessee, 1962.

6. Churchill, R. V., Modern Operational Mathematics in Engineering, McGraw-Hill, New York, 1944.

7. Clements, W. C., Jr., "Pulse Testing for Dynamic Analysis," Ph.D. Thesis, Vanderbilt University, 1963.

8. Clements, W. C., Jr., and Adler, R. J., Unpublished manuscript.

9. Clements, W. C., Jr., and Schnelle, K. B., Jr., Ind. Eng. Chem. Proc. Des. and Dev. 2, 94 (1963).

10. Elder, J. S., J. Fluid Mechanics, 5, 544 (1959).

11. Fischer, H.,"Longitudinal Dispersion by Velocity Gradients in Open Channel Flow," Technical Memorandum N. 64-4, W. M. Keck Lab. of Hydraulics and Water Resources, Calif. Inst. of Tech., 1964.

12. Godfrey, R. G., and Frederick, B. J., "Dispersion in Natural Streams," United States Department of the Interior, Geological Survey, Open-File Report, Washington, D. C., 1963.

13. Guillemin, E. A., Theory of Linear Physical Systems, Wiley and Sons, New York, 1963.

14. Hays, J. R., Clements, W. C., Jr., and Harris, T. R., "Model Evaluation in the Frequency Domain," A. I. Ch. E. Annual Meeting, Philadelphia, Pennsylvania, 1965.

15. Krenkel, P. A., and Orlob, G. T., J. Sanitary Engineering Division, ASCE, 88, 53 (1962).

16. Leonard, E. F., and Ruszkay, R. J., "Frequency, Transient and Moment Methods in Process Analysis," A. I. Ch. E. Annual Meeting, New York, 1961.

17. Marquardt, D. W., J. Soc. Indust. and Appl. Math. 11, 431 (1963).

18. Marquardt, D. W., Share General Program Library Share Distribution No. 1428 DFE 2135 (PA).

19. McKee, J. E., Lecture at Vanderbilt University, (December, 1965).

20. Mickley, H. S., Sherwood, T. K., and Reed, C. E., Applied Mathematics in Chemical Engineering, McGraw-Hill, New York, 1957.

21. Parker, F. L., J. Hydraulic Division, ASCE, 87, 151 (1961).

22. Schuster, J. C., J. Hydraulic Division, ASCE, 91, 101 (1965).

23. Spalding, D. B., "A Note on Mean Residence Times in Steady Flows of Arbitrary Complexity," Chem. Engr. Sc. 9, 74 (1958).

24. Taylor, G. I., Proc. Roy. Soc., A223, 446 (1954).

25. Taylor, G. I., Proc. Roy. Soc., A225, 473 (1954).

26. Thackston, E. L., "Longitudinal Mixing and Reaeration in Natural Streams," Ph.D. Thesis, Vanderbilt University, 1966.

27. Thomas, I. E., "Dispersion in Open Channel Flow," Ph.D. Thesis, Northwestern University, 1958.

28. Yotsukura, N., and Fiering, M. B., J. Hydraulic Division, ASCE, 90, 83 (1964).